



Historical Perspective

Viscoelastic properties of colloidal systems with attractive solid particles at low concentration: A review, new results and interpretations

Philippe Martinoty^a, Antoni Sánchez-Ferrer^{b,*}^a Institut Charles Sadron, UPR 22, CNRS/UDS, 23 rue du Loess, BP 84047, F-67034 Strasbourg, France^b Technical University of Munich, Wood Research Munich, Winzererstrasse 45, D-80797 Munich, Germany

ARTICLE INFO

Keywords:

Cluster fluids
Gels
Jammed systems
Colloids
RLCA
DLCA
RDLC
Percolation

ABSTRACT

This paper concerns the viscoelastic properties and the resulting structure of colloidal systems with short-range attractions in the regime where the volume fraction f is small. Unlike the high ϕ regime, which is well understood in terms of mode-coupling theory (MCT), the low ϕ regime is still the subject of a debate based on different concepts such as percolation, diffusion-limited colloidal aggregation (DLCA), jamming, or cluster mode-coupling approach. Prior to the analysis of three examples of attractive systems at low ϕ values, a summary of concepts relevant to understanding the formation and properties of such attractive particles is discussed in the present study. Afterwards, we re-analyze the behaviour at a low ϕ of i) suspensions of carbon black (CB) particles, ii) suspensions of poly(methyl methacrylate) (PMMA) hard spheres with a depletion attraction induced by the addition of polystyrene (PS), and iii) suspensions of amino acid organogelator molecules which form rod-like objects. The rheological properties of these systems have been studied in detail and their response has been interpreted as being due either to a solid network discussed in relation to the jamming state diagram or to a suspension formed by jamming of clusters. Our analysis shows that these three systems are in fact cluster fluids and that their solid-like response corresponds to a change in their viscoelastic response, the elastic component G' becoming greater than the viscous component G'' at low frequencies. Due to the presence of weak interparticle interactions in the tens range from 1 to 15 $k_B T$, a liquid-like state is reversibly achieved at high frequencies, as indicated by the crossover of G' and G'' as a function of frequency for a given concentration. Moreover, all these attractive particle systems at low ϕ show for both moduli a master curve which characterizes these cluster fluids and allows for the classification of these attractive particle systems.

1. Introduction and motivation

The study of systems exhibiting liquid-solid transitions is a field of research established for a long time. Research has focused on (a) crosslinked polymer systems, *i.e.*, chemical or physical networks in the melt or the swollen state [1–6], (b) repulsive colloidal systems, *i.e.*, repulsive hard spheres which give rise to a glass transition when the volume fraction ϕ is *ca.* 0.58 [7,8], and (c) attractive colloidal systems which are the subject of this article.

The attractive colloidal systems have long been used in everyday life, such as foods and cosmetics, in medical applications such as cartilage replacements, and in many industrial fields. They consist of weakly attractive particles dispersed in a solvent, which are initially separated but aggregate under suitable conditions to form clusters of a fractal nature, thus, leading to a colloidal network. These clusters come either

from the association of sticky hard spheres, *e.g.*, the widely studied octadecyl-coated silica particles [9–16], or from the association of colloidal particles resulting from a depletion mechanism [17,18], *e.g.*, colloid-polymer mixtures, for which the polymer concentration controls the attraction between colloidal particles [19–21].

Both the attractive colloidal systems and depletion systems exhibit a rich phase diagram which depends on the strength of the interparticle attraction U , the volume fraction of particles ϕ and the range of the attractive interaction ξ . They have been the subject of a large number of studies leading in particular to the understanding of their behaviour at high density values, which is characterized by the presence of two glassy states, *i.e.*, attractive and repulsive, separated by a fluid [19–21]. In contrast, the behaviour of these colloidal systems in low-density regimes is still poorly understood, although it has been extensively studied. These systems, which are characterized by a percolation-type formation

* Corresponding author.

E-mail address: sanchez@hfm.tum.de (A. Sánchez-Ferrer).<https://doi.org/10.1016/j.cis.2024.103335>

Received in revised form 28 October 2024;

Available online 8 November 2024

0001-8686/© 2024 The Authors. Published by Elsevier B.V. This is an open access article under the CC BY license (<http://creativecommons.org/licenses/by/4.0/>).

mechanism and a solid-type mechanical response, are often considered as solids immersed in a fluid or gel-like solids, although the existence of these gels has not been proven because the onset of gel formation - commonly called critical gel -, was not observed except in the case of octadecyl-coated silica particles suspended in *n*-tetradecane [13,14]. The elastic behaviour of colloidal systems has been reviewed [22], and their properties analyzed according to whether they were obtained in equilibrium or under non-equilibrium conditions [23].

The aim of this article is to shed new light on the origin of the solid-like behaviour of systems with weakly attractive particles in the low-density regime, by re-analyzing the mechanical behaviour of three different systems: (i) suspensions of carbon black (CB) particles [24–27], (ii) certain suspensions of poly(methyl methacrylate) (PMMA) spheres with a depletion attraction induced by the addition of polystyrene (PS) [26], and (iii) suspensions of amino acid organogelator molecules [28]. Our analysis shows that the solid-like response of these systems does not correspond to that of a jammed system but to a change in the viscoelastic response of a fluid of fractal clusters, which occurs when the elastic component G' of the shear modulus becomes greater than the viscous component G'' .

To place this study in the appropriate context, various theories and numerical simulations that have been used or proposed to describe the response of attractive colloidal systems in the low-density regime will be recalled: (a) the classical percolation of entropic nature - which is based on the fractal approach and introduces the particular properties of the critical gel making possible to identify a gel without any ambiguity -, (b) the elastic percolation and the rigidity percolation, (c) the diffusion-limited colloidal aggregation (DLCA) - which leads to the formation of a gel -, (d) the reversible diffusion-limited colloidal aggregation (RDLCA) - for which the gel state is not reached -, (e) the reaction-limited colloidal aggregation (RLCA) - which leads to the formation of an aggregated solid -, (f) the cluster mode-coupling approach - which is an extension of the mode-coupling theory (MCT) of glasses leading to a gel or an attractive glass -, (g) the spinodal decomposition, and (h) the jamming process - which leads to an amorphous solid. This is not a detailed review of this literature, but only a summary of concepts relevant to the understanding of the formation and properties of attractive systems discussed in the present study. This overview of the literature will also allow us to make a classification of the systems characterized by a solid-like response.

The article is organized as follows: Section 2 recalls the mechanisms controlling the formation and the mechanical behaviour of soft solids in Soft Matter. This section contains several subsections dealing respectively with classical percolation, elastic percolation, rigidity percolation, DLCA, RDLCA and RLCA mechanisms, jamming process and MCT applied to clusters. In Section 3, our analysis of the viscoelastic properties of carbon black suspensions, hard spheres suspensions with a depletion attraction induced by the addition of a polymer, and suspension of amino acid molecules leading to organogels is presented. Finally, our conclusions are summarized in Section 4.

2. Mechanisms controlling the formation and mechanical behaviour of soft solids in Soft Matter

Rheological measurements have always played a major role in determining the state of a system and its evolution as a function of parameters such as time, temperature or concentration because rheology macroscopically probes the response - liquid or solid - of the system (see for example the reviews on Soft Materials, including biological systems and cells [29], and those on liquid-crystal elastomers and gels) [30,31]. For equilibrium or quasi-equilibrium systems, they also provide a proper determination of the fluid-to-solid transition *via* the scaling law characterizing the critical gel, introduced for the first time for polymer systems [32,33]. This summary recalls the main rheology mechanisms that have been proposed to describe the formation and the mechanical behaviour of the different systems studied in Soft Matter. It includes the

different percolation approaches, the jamming approach, and the mode-coupling approach. In Table 1, a description for all soft solids described in Section 2, *i.e.*, polymer gels, colloidal gels, cluster fluids, colloidal aggregates, and jammed systems, is presented as a summary of the concept.

2.1. Percolation and basic definition of a gel

Many random materials exhibit important changes in their elastic behaviour as the degree of interconnection in the material increases. This behaviour change is usually explained by the concept of percolation, which is a critical physical process based on statistical considerations, allowing for the characterization of the behaviour of a set of incompletely connected objects for which long-distance communication is either possible or impossible depending on the number of objects and contacts between them. The transition from a random state with incompletely connected objects to a random state with connected objects is identified by the percolation threshold, which is the point where the parameter describing the connectivity takes a critical value. When this threshold value is crossed by continuously increasing the concentration of objects and/or their bonds, the system goes from a state of short-range connectivity to a state of long-range connectivity. The properties of the system then change abruptly at this point, and the percolation transition behaves like a second-order phase transition in connectivity. The theory of percolation, therefore, belongs to the framework of phase transitions. It has been applied to the description of numerous systems of Solid-State Matter and Soft Matter, the polymeric and colloidal systems are the most representative in the field of Soft Matter. This subsection will focus on the two different percolation models, *i.e.*, classical and elastic, which correspond to the usual approaches of gelation theory.

2.1.1. Classical percolation and electrical analogy

As we have just recalled, gelation is the phase transition from a state composed of molecules - monomers - and finite clusters formed by some of these molecules, towards a gel, which is a state presenting an infinite network formed by a macromolecule of infinite size. This assumes that the gel forms continuously, meaning there is no phase separation and that the gel fraction vanishes continuously at the gel point. The sol-gel transition is therefore a continuous transition that behaves like a second-order phase transition in connectivity [3–5]. This description applies to gels formed from a solvent-free melt (undiluted gels). The situation may be different for gels formed from solutions since, depending on the chemical potential, the gel fraction may either vanish continuously at the gel point or may jump to zero discontinuously if the system jumps over the miscibility gap. In the language of phase transition theory, this second situation is called a first-order transition, which is characterized by a region where the phases before the transition and after the transition coexist. The evolution of the system in this coexistence region is governed by a nucleation and growth mechanism. Regarding the polymer systems discussed here, it should be noted that their final structure strongly depends on the way they are formed. This is illustrated in Section 3.2 - Colloidal suspension of hard spheres (PMMA) with depletion interaction -, which deals with colloidal systems with very low colloidal volume fraction and different polymer concentrations for which the nucleation and growth process and the mechanisms leading to a first- or second-order sol-gel transition provide a good description of the final structure of these different systems.

2.1.1.1. Gels formed from a solvent-free melt or undiluted gels. The percolation model is a particular approach to gelation. It can simply be explained by assuming that the monomers occupy the sites of a periodic lattice and that between two nearest neighbours of the lattice sites, a bond is formed randomly with a probability p . If p is close to zero, most of the sites are isolated, except for a few pairs or triplets of sites. When p

Table 1
Classification, mechanism of formation and characterization of some soft solids.

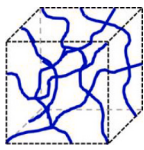
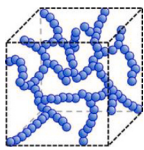
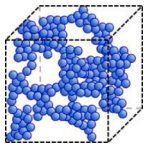
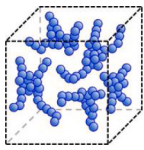
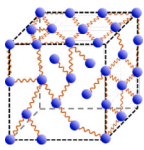
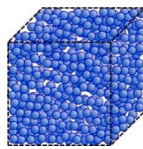
Chemical and physical polymer gels formed by entropic percolation		<ul style="list-style-type: none"> • Chemical gels by chemical crosslinking (<i>i.e.</i>, covalent bonds) • Physical gels by physical crosslinking (<i>i.e.</i>, ionic bonds, hydrogen bonds, crystalline domains, entanglements, π-π stacking) • 2nd-order phase transition in connectivity (the observation time must be longer than the dynamics of the physical gel formation) • Existence of a critical gel • Presence of a gel point: $G'(\omega) \sim G''(\omega) \sim \omega^3$ • Master curve • Fractal formation of colloidal clusters
Colloidal gels formed by diffusion-limited colloidal aggregation (DLCA)		<ul style="list-style-type: none"> • Growth process: $G' \sim (\phi - \phi_{gel})^1$ • Existence of a critical gel • Presence of a gel point: $G'(\omega) \sim G''(\omega) \sim \omega^3$ • Master curve
Aggregated colloidal solids formed by reaction-limited colloidal aggregation (RLCA)		<ul style="list-style-type: none"> • Solid formed far from the gelation threshold when $G' > G''$ (no percolation transition) • A collection of tightly packed fractal aggregates throughout the sample • Growth process: $G' \sim \phi^u$ • No existence of a critical gel (unlike the colloidal gel)
Fluid of colloidal clusters resulting from reversible diffusion-limited colloidal aggregation (RDLCa)		<ul style="list-style-type: none"> • Fractal formation of colloidal clusters with a finite inter-particle attraction energy • Cluster fluid that depends on the bond energy U • Growth process: $G' \sim (\phi - \phi_c)^1$, where ϕ_c is the percolation threshold (when U is high, but not high enough to lead to an irreversible growth process) • No existence of a critical gel (there is no gelation process) • Master curve • Cluster mode coupling approach can also lead to a cluster fluid
Elastic percolation networks		<ul style="list-style-type: none"> • A vectorial percolation model where contact interactions between particles produce geometric connections • Growth process: G' and G'' follow a critical behaviour as a function of $(p - p_{c,elastic})$, where $p_{c,elastic}$ is the percolation threshold • Critical values of exponents: different from those of scalar percolation • Main models: i) Central-Force (CF) model - rigid framework formed of elastic connections or springs with only stretching forces, ii) Bond-Bending (BB) model with a bond-bending term added to the elastic network energy - stretching and bending forces are present

Table 1 (continued)

Jammed systems (at zero temperature)		<ul style="list-style-type: none"> • Jamming occurs when all the particles touch • Attractive systems formation: two 2nd-order transitions - first a connectivity transition from a non-percolated state (liquid-like) to a percolated but unjammed state (gel-like), followed by a rigidity transition from the percolated state to the jammed state (critical point J) • Repulsive systems formation: one 1st-order rigidity transition at point J from the non-percolated state to the jammed state • Jamming transition at point J for attractive systems: $G' \sim (\phi - \phi_c)^2$ • The jammed state is the most disordered of states (crowding of the space or random close-packing density)
--------------------------------------	---	--

increases, small clusters form and connect themselves to form larger clusters. For a critical probability p_c , an infinite cluster appears, which extends from one end to the other of the lattice, which indicates the formation of the gel. The critical probability p_c is named the percolation threshold. It indicates that a phase transition occurs between a state without a gel structure for $p < p_c$, and a state with a gel structure for $p > p_c$. Beyond p_c , as $p \rightarrow 1$, most of the very large clusters become infinite clusters that contribute to the gel formation, the remaining finite clusters and remaining monomers being trapped inside the gel. A gel is therefore a solid, which usually coexists with a sol formed for unreacted monomers, oligomers and unconnected clusters.

Since the percolation model is a continuous phase transition model (no phase separation) [3,4], the scaling concepts for the thermodynamic of a second-order phase transition were introduced to describe the behaviour of the system in the asymptotic region around the gel point (*i.e.*, around p_c) where the critical phenomena occur. Note that the percolation model is scalar in nature and is generally based on a lattice, but the percolation model based on a continuum (*i.e.*, without a lattice structure) presents in two and three dimensions the same exponents inside the error bars [34–36], which indicates that the lattice is not an important parameter.

A well-known example of percolation is given by the formation of solvent-free chemical polymer gels, which are characterized by covalent and, therefore, permanent crosslinks connecting the polymer backbones in a three-dimensional lattice. Historically, modelling of the formation of a chemical polymer gel was initiated by Flory [37,38] and Stockmayer [39,40], whose description assumes that each bond between two monomers is formed randomly, but ignores cyclic bonds - closed loops formation -, excluded volume and steric hindrance effects. It is essentially equivalent to a random bond percolation process performed on a tree-like structure, the Bethe lattice or Cayley tree. Later, Stauffer [41] and de Gennes [42] underlined the role of loops, excluded volume and steric hindrance, which were not taken into account in the tree-like description, and proposed to replace it with percolation on three-dimensional (3D) lattices. de Gennes also proposed that the shear modulus G of the gel varies with the conductivity of a random mixture of conductors (fraction p) and insulators (fraction $1-p$) [42], and that the viscosity η of the sol varies with the conductivity of a random mixture of superconductors (fraction p) and normal conductors (fraction $1-p$) [43]. As for the classical percolation, the electrical analogy model is a scalar percolation, which is independent of the type, bond or site of the

percolation mechanism that concerns solvent-free systems. Although the behaviour of some polymeric materials can be described by the electrical analogy model [44], it has appeared that more general models are needed to understand the elasticity of several other random percolation networks. This gave rise to the development of the elastic percolation models which are described in Section 2.1.2.

The dynamics of the percolation theories reviewed in the previous paragraph have been ignored. However, this is an important aspect of gelation theory since the probability of bond formation is not necessarily random but may depend on various parameters such as molecular mobility.

A viscoelastic theory based on the 3D percolation model has been developed to describe the behaviour of a polymer system near the sol-gel transition [45,46]. In the hydrodynamic limit, it shows that the shear modulus G' and the shear viscosity η vary according to the following critical laws: $G' \sim (p - p_c)^t$ for $p > p_c$ and $\eta \sim (p_c - p)^s$ for $p < p_c$, where t and s are the critical exponents of elasticity and viscosity, respectively.

The knowledge of p_c is of crucial importance for the determination of the critical exponents, since the critical laws depend on $(p - p_c)$. An accurate determination of p_c is obtained from the behaviour of G' and G'' as a function of the frequency ω , which shows that both components of the shear modulus follow the same power law $G'(\omega) \sim G''(\omega) \sim \omega^n$ when $p = p_c$ [32,33], where n is the relaxation exponent - the viscoelastic exponent. This behaviour reflects the fact that critical gel - or incipient gel - is due to a self-similar distribution of self-similar clusters, from monomers to an infinite cluster. Moreover, n is given by the relation $n = t/(t + s)$ with $t = d - \nu$, where d is the spatial dimension and ν the exponent of the correlation length ξ , which varies as $\xi \sim (p - p_c)^\nu$.

The evolution of the rheological behaviour near the sol-gel transition comprises three different regimes: a) a pre-critical regime (below the gel point, when $p < p_c$), for which $G'(\omega) < G''(\omega)$ and approach each other when p increases; b) a critical regime (at the gel point when $p = p_c$) for which $G'(\omega)$ and $G''(\omega)$ become parallel; and c) a post-critical regime (above the gel point, when $p > p_c$) for which G' and G'' separate without intersecting in the gel region with $G'(\omega) > G''(\omega)$. It has to be noted that this evolution assumes the absence of interference between gelation and glassy behaviour.

The power law behaviour of G' and G'' at the gel point results from the fact that the critical gel corresponds to a distribution of fractal clusters, from monomers to infinite clusters. The exponent n is, therefore, linked to the fractal dimension d_f , which characterizes the geometrical structure of the gel, as we will see later. The determination of the critical gel is a key point in the dynamics of an incipient solid because it allows determining without ambiguity if the solid is a gel or not, and, in the case where the solid is a gel, an accurate value of the critical exponents s and t .

The exponents n , s and t depend on the microstructure of the percolating polymer - entanglement effects, hydrodynamic and excluded-volume interactions. For a polymer without entanglement and hydrodynamic interactions, which corresponds to a Rouse behaviour, n , s and t are given by $n = d/(d_f + 2)$, $s = \nu \cdot (d_f + 2 - d)$, and $t = d - \nu$, with $d_f = 2.5$ for $d = 3$ and $\nu \approx 0.88$ - the commonly accepted value in 3D - [3,5,47], n , s and t become $n \approx 0.67$, $s \approx 1.33$ and $t \approx 2.66$. When the excluded volume and hydrodynamic interactions are both completely screened out, n is given by $n = d \cdot (d + 2 - 2d_f) / [2(d + 2 - d_f)]$ [48].

For the electrical analogy model, the exponents s and t were calculated by numerical methods *via* the ratios t/ν and s/ν [49,50]. From the values of $t/\nu \approx 2.2$ [49] and $s/\nu \approx 0.85$ [50], and with the value of $\nu \approx 0.88$, one obtains $t \approx 1.94$ and $s \approx 0.75$, and the corresponding value of $n = 0.72$. Moreover, a $t/\nu \approx 0.97$ [50,51] was also calculated for a 2D percolation system leading to a value of $t \approx 1.29$ when $\nu = 4/3$.

It should be noted that the analogy between elasticity and the growth of the conductivity in a random resistor network has raised theoretical controversies due to the fact that the lattice used has an elastic energy E which is not rotationally invariant [52,53]. However, as noted by Alexander [54], the de Gennes' model could be justified by the presence

of internal or external stresses to which the gels would be subjected leading to a critical exponent of the elastic modulus equal to that of the conductivity near the percolation threshold. In other words, scalar percolation would be predominant near the gel point. This question now seems settled in view of the scaling results from Yu et al. [55] on the fractal nature supporting de Gennes' approach.

In summary, the triad (n , s , t) has values of (≈ 0.67 , ≈ 1.33 , ≈ 2.66), (≈ 1 , 0 , ≈ 2.66) and (≈ 0.72 , ≈ 0.75 , ≈ 1.94), when considering respectively no hydrodynamic interactions - Rouse model -, hydrodynamic interactions - Zimm model for which the viscosity increases logarithmically, and $s = 0$ -, and the electrical analogy model in 3D.

A critical gel has been observed in various chemical systems cross-linked in the melt (no solvent present), such as epoxy resins [46,56-62], polyurethanes formed by radical polymerization [63-65], polycaprolactone [66], polystyrene [67], poly(dimethylsiloxane) (PDMS) [32,33,68], polybutadiene [69], polyester [70,71], and silyl-terminated poly(propylene oxide) [72]. Since the critical gel is the key property of a gel, these systems can therefore be referred to as gels without any ambiguity.

The universality of dynamics exponents can be tested by comparing the value of n measured at the critical gel to the calculated value n_{calc} from the measured exponents s and t using the relation $n = t/(t + s)$. However, measurements of the three exponents n , s and t taken in the same experiment are very few. They have been measured for one-component epoxy-resin of a molar mass of 290 Da ($n = 0.64$, $s = 1.33$, $t = 2.26$ and $n_{\text{calc}} = 0.63$) [60], two-component epoxy resin of molar mass 202 and 204 Da ($n = 0.70$, $s = 1.44$, $t = 2.65$ and $n_{\text{calc}} = 0.65$) [58], two-component polyester of 146 and 134 Da ($n = 0.66$, $s = 1.36$, $t = 2.71$ and $n_{\text{calc}} = 0.67$) [70] and for a silyl terminated poly(propylene oxide) of 2000 Da ($n = 0.67-0.68$, $s = 1.3$, $t = 2.0-2.1$ and $n_{\text{calc}} = 0.61-0.62$) [72]. For the epoxy and polyester gels, there is good agreement between both n and n_{calc} values, and between the n_{calc} values of the different samples suggesting that the exponents are of the Rouse-type ($n \approx 0.67$, $s \approx 1.33$, $t \approx 2.66$). The Rouse behaviour indicates that the chains between the crosslinking points are short and with no entanglement - degree of polymerization $DP \approx 1$ -, which is the case for these systems. In contrast, the data obtained for the end-linking poly(propylene oxide) gel shows that n_{calc} is different from the Rouse n value. This results from the measured value of $t = 2.0-2.1$ which is not of Rouse-type, unlike the measured values of n and s . Moreover, this small value of t is also incompatible with the Rouse-type value ($t = 2.7-2.8$) deduced from the steady state compliance below the gel point. These seemingly contradictory results have been explained by suggesting that the critical exponent of the equilibrium modulus is mainly due to links in the backbone, whereas, in addition to the links in the backbone structure the blobs and dangling chains embedded in the cluster contribute to the steady state compliance [72].

Note that there are many experiments performed on low DP systems leading to gels with a value of n around 0.7 (e.g., $n \approx 0.70$ [45] and $n \approx 0.71$ [57,62] for epoxy, $n \approx 0.70$ [65] for polyurethane, $n \approx 0.69$ [71] for polyester) lying between the value of the Rouse percolation model ($n \approx 0.67$) and the value of the electrical analogy model ($n \approx 0.72$). Whether these gels fit the Rouse model or the electrical analogy model has hotly been debated for many years, but with answers that are not always clear because the two values of n are not far from each other, and the exponents s and t were not measured in these experiments. However, epoxy gel [58,60] and polyester gel experiments [70] indicate that the percolation mechanism of these gels is of the Rouse type, although the value of some of their exponents is not exactly that expected for the Rouse model. This suggests that the behaviour of the epoxy gels [45,57,62], of the polyurethane gel [65] and of the polyester gel [71] could be described by the Rouse model too.

When DP increases, the values of n are no longer in agreement with the Rouse-type behaviour and decrease as DP increases. This is for example illustrated by values of n as low as $n \approx 0.2$ observed for very long chains between the crosslinking points [68], as well as by a

decrease in n from 0.5 to 0.2 as DP increases from 20 to 141 [67]. As suggested by Lusihan et al. [70], these low values of n are probably due to entanglements between the long chains connecting the crosslinking points (large DP), which invalidates Rouse's percolation model. Therefore, n is an exponent which is not universal but depends on the values of DP. n becomes universal within the limit $DP \approx 1$, i.e., for short chains between the crosslinking points, which corresponds to the Rouse-type percolation.

Finally, it should be noted that percolation has been used successfully to describe the sol-gel transition as a function of the extent of the reaction by applying appropriate vertical and horizontal shifts to the G' and G'' values at different stages of the reaction, thus reflecting the change in connectivity [61].

2.1.1.2. Gels formed from a solution. So far, the gels we have considered are solvent-free systems like polymer melts or reactive monomers. These systems can be described by random-bond percolation or electrical analogy models for which each site is occupied by a monomer, and bonds between monomers are randomly formed to build up clusters. However, many gels form in a solvent. To describe these dilute gels, the concept of percolation has been extended to situations where solvent molecules are also present in the sol phase. In this case, the sites are occupied either by a monomer with a probability ϕ - molar fraction - or by a solvent molecule with a probability

$(1-\phi)$. As a result, the two nearest neighbouring monomers can form a bond with probability p , while no bond leads to or originates from solvent molecules. The original model of random percolation of bonds is thus transformed into a random percolation model of the site-bond type, in which the clusters are formed of randomly distributed monomers linked by random bonds. This change from bond percolation to site-bond percolation has no consequence on the values of the critical exponents.

These dilute gels, however, have some differences compared to solvent-free gels. The first is that clusters swell when diluted in a good solvent, causing their fractal dimension to change. In 3D, the fractal dimension decreases from $d_f \approx 2.5$ for the undiluted or melt regime - the percolation model - to $d_f \approx 2$ for the dilute regime - lattice animal model [73,74]. This decrease results from the fact that the intra-cluster interactions are partially screened for the undiluted regime, whereas, they are unscreened under dilution, and the excluded volume interactions are strong. In the diluted regime, the exponents are those of the random bond percolation [75–78], but this is no longer the case in the semi-diluted regime which occurs when the concentration C is greater than the concentration C^* for which the polymers come into contact. The crossover concentration C^* separating the diluted and semi-diluted regimes was calculated as a function of the mass average molar mass M_w [79].

Other complications can arise, such as a possible competition between gelation and phase separation as noted previously, or hydrodynamic interactions which can have significant effects on the rheological properties, even if the static properties are modeled by classical percolation.

In dilute solutions, the attracting monomers diffuse and collide to bind irreversibly, thus leading to the formation of larger clusters. This kinetic process generates a state of non-equilibrium, which cannot be described by the equilibrium percolation models mentioned above. This process depends on the conditions of formation of the clusters: diffusional-limited colloidal aggregation (DLCA) for a rapid aggregation process, i.e., when bonds form just after a few collisions; and reaction-limited colloidal aggregation (RLCA) for a slow aggregation process. The two processes differ, in particular, by the fractal dimension of the clusters and the nature of the resulting system.

Examples illustrating the growth of a gel under dilute solution are given by alcogels resulting from dilute solutions of tetramethyl orthosilicate (TMOS) in methanol-water mixtures with a base catalyst [80] and from dilute solutions of tetraethyl orthosilicate (TEOS) in ethanol-

water mixtures with an acid catalyst [81,82]. In both cases, a critical gel is observed showing that the resulting solid is a gel. The (n, s, t) values were measured for the TEOS gel ($n = 0.72, s = 0.88,$

$t = 2.2$ and $n_{\text{calc}} = 0.71$) and can be considered to be in reasonable agreement with the electrical percolation model.

The formation of TMOS and TEOS gels, or similar dilute gels, takes place in two steps. In the first step, the fractal colloidal clusters grow exponentially due to their aggregation. This is the RLCA regime. In the second step, which occurs when these colloidal clusters become large enough to fill the available volume of the solution (i.e., overlapping of the clusters), the system crosses over to the critical growth associated with gelation. This is the DLCA regime. It is only valid near the sol-gel transition and, as noted above, cannot describe spatial correlations that develop long before the sol-gel transition and are due to aggregation occurring at early times. By monitoring the kinetics of growth, it is possible to favour either the DLCA regime or the RLCA regime, as has been shown on the TMOS system (DLCA regime [83], RLCA regime [84]).

Finally, it should be noted that systems made up of small attractive molecules - monomers - in dilute solution, such as the TMOS or TEOS systems, have many points in common with systems made up of solid particles, e.g., gold particles, introduced in an appropriate solvent. The behaviour of such systems will be discussed in Section 2.2, since in both cases the formation of the solid system is based on the DLCA or RLCA regimes. However, they differ in that the colloidal particles resulting from the association of monomers are formed in the reaction and are not added to the reaction bath as in the case of solid colloidal particles.

The percolation theory also applies to physical systems for which the gel is formed continuously, with a lifetime of the junctions between the constituents of the system longer than the experimental observation time. Like for chemical polymer systems, critical gels have been observed in various physical polymers systems, the most studied systems being poly(vinyl chloride) (PVC), and biopolymers, showing that the sol-gel transition in these systems is a second order transition in connectivity [6,85–95].

As a consequence, the formation of a physical polymer gel does not result from a first-order sol-gel transition, as asserted in several places in the two books on physical gels [96,97]. This misconception of what a physical polymer gel is leads to incorrect claims such as: (i) a physical polymer gel is distinguished from a chemical polymer gel by the order of the sol-gel transition, namely a first-order transition for the physical polymer gel and a second-order transition for the chemical polymer gel. As the experimental results just referenced show, a continuously formed physical gel is not characterized by a first-order transition. The first-order phase transition only occurs in certain systems for which there is competition between gelation and phase separation leading to a coexistence region. The resulting solid is, therefore, not characterized by an infinite network, thus, it is not a gel although it is called so. (ii) There is no specific theory on the mechanical properties of physical gels. This statement does not apply to physical gels resulting from a second-order phase transition, whose mechanical properties can be explained by the percolation model, as for chemical gels. However, this statement applies to physical gels associated with a first-order phase transition arising from a competition between gelation and phase separation. In that case, the theory will depend on chemical potential. (iii) The transition temperature T_{gel} is given by the DSC experiments, whereas the sol-gel transition is not thermodynamic but connective in nature. The DSC experiments only give the temperature, T_{DSC} , associated with the formation of the clusters at the origin of the gel. A rigorous determination of T_{gel} is given by the congruent behaviour of G' and G'' at the critical gel as mentioned above. The difference between T_{gel} and T_{DSC} can be very large ($> 35^\circ\text{C}$) when the concentration in the reactant is relatively small and gradually decreases when the concentration in the reactant increases [89].

2.1.2. Elastic percolation

In the percolation models, which have just been recalled, the elasticity of the gel results from a mechanism of connectivity due to a scalar or isotropic nature alone. These percolation models describe well most of the sol-gel transitions of gels made up of branched and flexible polymer chains where entropic effects dominate. However, for other random network systems, the scalar or isotropic percolation is not sufficient to transmit the stresses and another type of model, called elastic percolation, has been developed to describe the elastic properties of random networks near the percolation threshold. This elastic percolation model represents a new class of percolation, where geometric connections, such as contact interactions between pairs of macroscopic particles, involve elastic connections. As for scalar percolation, the shear elastic modulus and viscosity follow a critical behaviour as a function of $(p - p_{c,elastic})$, where p is the fraction of active bonds and $p_{c,elastic}$ the percolation threshold, but with the corresponding exponents T - for the shear modulus - and S - for the viscosity - which are different from those of the scalar percolation t and s , respectively. More precisely, for $p > p_{c,elastic}$, the shear modulus G varies as $(p - p_{c,elastic})^T$, and the correlation length ξ diverges as $(p - p_{c,elastic})^{\nu_{elastic}}$, and for $p < p_{c,elastic}$, the viscosity η varies as $(p - p_{c,elastic})^S$, where the parameters T , S , $p_{c,elastic}$ and $\nu_{elastic}$ depend on the type of forces associated with the formation of the network.

Elastic percolation is a vectorial approach to percolation that is based on computer simulations. There are different types of elastic percolation, depending on the interaction energy E . We focus here on two elastic percolation models, namely the central-force (CF) model [53,98–109], and the bond-bending (BB) model [52,110–120], which have been widely studied and exhibit very different critical elastic behaviours.

The CF percolation model corresponds to the case where each bond represents an elastic element, or a spring, which leads to a network with a rigid backbone formed by elastic bonds or springs, for which only stretching forces are present. E represents, therefore, the energy required to change the length of a bond. This CF percolation model is rotationally invariant. It is sometimes called “rigidity percolation” to distinguish it from the class of universality “elastic percolation” mentioned above.

Numerous numerical simulations were carried out to characterize this CF percolation model [53,98–103]. For both 2D and 3D systems, the simulation of bond percolation revealed that $p_{c,CF} > p_c$, and $T > t$ which has led to suggest that the CF elastic percolation and the conduction percolation do not belong to the same universality class [98].

More accurate simulations of bond percolation in 2D and 3D were carried out subsequently, in particular, to determine the values of T/ν_{CF} because the latter combined with the value of ν_{CF} makes it possible to deduce T . For 3D CF simulations, $T/\nu_{CF} \approx 2.2$ [99,100], and with $\nu_{CF} \approx 0.88$ [47], $T \approx 2.00$. For 2D CF simulations, $T/\nu_{CF} \approx 1.35$ [101–103], and $\nu_{CF} \approx 1.05$ [53,102], which gives $T \approx 1.42$. On the other hand, the value of the conductivity exponent t in 3D is $t \approx 1.94$ ($t/\nu \approx 2.2$ [49], $\nu \approx 0.88$) [47] and $t \approx 1.30$ in 2D ($t/\nu \approx 0.97$, $\nu \approx 4/3$) [51]. Therefore, the comparison between the conductivity exponent t and the CF exponent T shows that $T > t$ is for both 3D and 2D bond percolation. Likewise, the comparison between ν_{CF} and ν ($\nu \approx 0.88$ and $\nu \approx 4/3$ for 3D and 2D bond percolation, respectively) shows that $\nu_{CF} < \nu$ for each type of bond percolation. In summary, $T \geq t$ and $\nu_{CF} < \nu$ for both 3D and 2D bond percolation.

It has also been established that the topological properties of the elastic percolation clusters differ from those of classical percolation clusters [103], and that the critical exponent T/ν_{CF} and the threshold $p_{c,CF}$ depend on the type of percolation process, as shown by the results obtained on 2D systems. For example, $T/\nu_{CF} \approx 1.42$ and 1.14 for bond and site percolation, respectively [101]. The fact that T/ν_{CF} depends on the type (bond or site) of the percolation process indicates that the CF percolation depends on the microscopic details of the system, and, therefore, does not exhibit universal scaling laws, unlike scalar percolation for which T/ν_{CF} and $p_{c,CF}$ do not depend on the type of percolation

process. The CF percolation model has also been studied on 2D systems by an effective-medium approximation, with results in agreement with the simulation studies [104–109].

The second type of elastic percolation model corresponds to the case where a bond-bending term is added to the network energy, creating angular forces between the bonds, which become elastic elements that can be stretched and bent, as in covalent glasses. This percolation model corresponds to a vectorial approach and is called the bond-bending (BB) model. Like the CF model, it is based on computer simulations and is rotationally invariant. BB percolation was studied on 2D [110–116] and 3D [117] systems and was compared to the corresponding 2D and 3D CF percolation [52]. These studies show a) that the percolation threshold of the BB percolation is the same as that of the scalar percolation, b) that the bonds and sites of the BB percolation give the same result as the scalar percolation, and c) that the value of the critical exponent T of the shear modulus is $T \approx 3.75$ in agreement with the value deduced from the relation $T = t + 2\nu$, where t is the critical exponent of the electrical analogy and ν the exponent of the correlation-length in 3D. This shows that the BB model has universal scaling properties, unlike the CF model. As in the case of scalar or isotropic percolation, BB percolation is characterized by a critical gel [13,14].

Systems for which the contribution of BB forces is important have been observed on systems for which chemical reactions play no role. This is the case with randomly perforated metal sheets [118], powders [119], silica aerogels [120], and with some colloidal suspensions for which the value of T is greater than t as will be shown in the Section 2.2.

2.1.2.1. Continuous deformation of random networks. As already discussed, scalar percolation occurs before BB percolation. In this regard, experiments carried out in certain systems [121–123] have shown that the formation of the gel results from a percolation mechanism in agreement with the electrical analogy model, and that it is followed far from the threshold of this percolation by a second percolation consistent with the BB model, thus reflecting a change in the nature of the elasticity of the gel as it moves away from the scalar threshold.

This behaviour change can be explained by using the approach developed in the context of the continuous deformation of random network materials [124–126] which is based on the covalent energy mentioned above containing the bond-stretching and bond-bending terms. It does not deal with the formation of a random network but with its deformation by following the evolution of the average coordination number $\langle r \rangle$ [124–126]. For small $\langle r \rangle$ values, the network which results from a connectivity percolation of local flexible units is a soft solid characterized by large soft and floppy regions with some rigid inclusions, which reflects the random nature of the network (but does not indicate that the material is a two-phase material). As $\langle r \rangle$ increases, the small rigid regions grow larger until they percolate at $\langle r \rangle \geq r_p = 2.4$ [126], transforming the soft solid with floppy inclusions into a rigid solid. This shows that a transition from a soft to rigid solid occurs when network connectivity increases, but not in the classical sense of a transition between two phases. This topological approach can be applied to the gel, which confirms that there is a transition between a soft gel and a rigid gel, with a threshold p_r greater than the percolation threshold of connectivity p_c , but it does not give any information on the formation of the gel in terms of percolation mechanism and critical exponents.

2.1.2.2. Entropic elasticity. An important question concerns the role of temperature, since the CF and BB models in 2D and 3D described above, were made for an absolute temperature value of 0 K, whereas the experiments are carried out at temperatures above 0 K. Simulations showed that for $T > 0$ K there is an important contribution to the shear modulus that is entropic in nature [127–130]. In particular, Plischke et al. showed that these systems are rigid for all $p > p_c$ and that near p_c the shear storage modulus $G' \sim (p - p_c)^t$, where the exponent $t \approx 1.3$ and $t \approx 2$ for 2D and 3D lattices, respectively [128]. These results support the

conjecture of de Gennes that the diluted central-force network is in the same universality class as the random resistor network. The experiments mentioned above [123] support this result since the reported value of the exponent is $t = 2.0$ in a very narrow region close to the gel point, which is close to the conductivity percolation exponent $t \approx 1.94$ as for the other exponents.

2.2. Colloidal association: gels, aggregated solids, fluids of clusters and jammed systems

As recalled in Section 2.1.1, chemical and physical polymer gels are the results of a connectivity mechanism based on scalar or isotropic percolation models. However, there are also colloidal systems under dilute conditions, whose formation can be described by the elastic percolation models. Colloidal systems are defined as resulting from interactions of solid particles suspended in a solvent, the size of which is generally between approximately 10 nm and a few microns. The solid particles diffuse through the fluid medium, collide and bond continuously to form small clusters. These also diffuse through the fluid medium, collide and bind together to form larger clusters, and so on. This hierarchical growth of clusters is similar to that relative to systems consisting of small attractive molecules suspended in a solvent and which aggregate in the reaction bath, such as the case for TMOS and TEOS systems mentioned in Section 2.1.1. The formation and structure of the resulting solid depend on the concentration ϕ of the colloidal particles but also on the nature of their interaction.

When the solid particles interact only by volume exclusion, the crowding of the particles by their neighbours increases when ϕ increases leading to the formation of a glass (hard-sphere interaction). Typical examples of colloidal glasses are given by suspensions of uncoated silica (SiO₂) spheres in ethylene glycol [131], PMMA spheres stabilized sterically by thin layers of poly(12-hydroxystearic acid) (PHSA) dispersed either in a mixture of decalin and carbon disulphide [7,8] or in a mixture of *cis*-decalin and cycloheptyl bromide [132], or in dodecane [133], and clay particles (Laponite) in aqueous suspension at low ionic strength values [134–138].

When the interaction between solid particles is attractive, the formation of fractal clusters may be due to either the association of sticky hard spheres, *i.e.*, octadecyl-coated silica particles [10–16], or the association of repulsive colloidal particles, *i.e.*, particles interacting with volume exclusion, resulting from a depletion mechanism [17,18], as for colloid-polymer mixtures for which the polymer concentration controls the attraction between the colloids [19–21]. The nature of the resulting network depends on the formation mechanism (DLCA or RLCA), as it will be discussed in the following subsection.

2.2.1. Diffusion-limited colloidal aggregation (DLCA) and reaction-limited colloidal aggregation (RLCA) mechanism

The DLCA and RLCA regimes of colloidal systems have been studied by computer simulations [139–152], as well as by experiments carried out on numerous systems made up of solid particles, such as suspensions of gold particles [153–158], silica particles [9–16,84,121,123,158–169], and polystyrene particles [158,170–174].

The DLCA regime corresponds to conditions of rapid growth with open and tenuous clusters characterized by a fractal dimension $d_f \approx 1.7$ – 1.8 [2,13,155,158,161,167,170] in agreement with computer simulations [152]. In this process, the fractal clusters develop until they are large enough to fill the volume of the container. Then, the clusters become practically immobilized and behave like large particles that randomly bond to neighbouring particles, thus leading to a crossover from the growth process to the process of static percolation. This change of regime corresponds to the critical gel, which is characterized by $G'(\omega) \sim G''(\omega) \sim \omega^n$ where ω is the frequency and n the relaxation exponent, as it was recalled in Section 2.1.1. A critical gel was observed and characterized in several works for particles added in the reaction bath [12–14] and for particles formed in the reaction bath [81,82,121,123].

Since the colloidal systems resulting from the DLCA mechanism are gels, their mechanical properties can be characterized by a master curve, by applying vertical and horizontal shifts to the individual data sets, like for polymeric systems [2]. Two master curves are required: one associated with the sol phase and the other with the gel phase. In general, the horizontal shift is sufficient to construct the master curve. However, a vertical displacement of the curves is sometimes necessary, for example, when the density variation is significant or when the strong adhesion on the glass slides carrying samples of certain complex polymer systems such as a nematic monodomain of side-chain liquid crystal elastomer – and shape memory materials in general – does not allow them to adapt their length to temperature variations [175].

Although there are many colloidal systems formed by solid particles for which $G' \sim (\phi - \phi_{gel})^t$, few of them can be assimilated into a gel. This is because the critical gel, which marks the onset of gel formation, has not been determined. An exception is the system formed by octadecyl-coated silica particles suspended in *n*-tetradecane [14]. The presence of a critical gel has also not been reported in depletion systems formed by colloid-polymer mixtures [26], so it is not certain that these systems are gels. To our knowledge, there is no depletion system for which a critical gel has been observed.

The RLCA process corresponds to slow growth conditions for which many collisions between clusters occur before bonding. Experiments show that RLCA is characterized by a fractal dimension $d_f \approx 2.0$ – 2.1 [9,10,84,154,158,160,161] in agreement with computer simulations [139–152], which indicates that the RLCA clusters are more compact than the DLCA clusters. On the other hand, DLCA and RLCA depend on the growth kinetics as has been shown on suspensions of gold, silica and polystyrene particles [158], as well as in the case of the TMOS and TEOS systems.

As for non-colloidal gels formed in solution, the colloidal gel formation takes place in two stages. The first stage is the RLCA regime for which the fractal colloidal clusters (often called flocs) grow exponentially *via* cluster aggregation. These non-equilibrium clusters continue to grow until the solution reaches the semi-dilute condition, where the clusters fill the volume of the container. At this point, the dense solution of clusters crosses over to the critical growth leading to the gel, and the system is in the DLCA regime. This formation process indicates that the final structure of the gel does not depend on the behaviour near the gel point, but on the cluster growth that occurred at the earliest times in the RLCA regime. The time for the gel formation depends on the growth kinetics. This time becomes very long when the RLCA process is too slow – sometimes several days –, so that one can say that DLCA forms a gel in a “finite time” whereas RLCA takes an “infinite time”.

In the RLCA regime, the scaling behaviour of the elastic properties of the solution is characterized by a growth process of G' given by $G' \sim \phi^\mu$ [63,166,168,169,171,174]. This growth process of G' has also been obtained by assuming that the structure of the colloidal network is analogous to that of a polymer gel [174]. This approach, which consists of replacing the blobs of the polymer gel with the colloidal flocs formed during the formation of the colloidal network, takes into account the fact that the interfloc links can be weaker – weak-link regime – or stronger – strong-link regime – than the stiffness of the flocs. As a result, the exponent μ is given by $\mu = (3 + x)/(3 - d_f)$ for the strong-link regime, and by $\mu = 1/(3 - d_f)$ for the weak-link regime, where x is the backbone fractal dimension of the flocs. There are very few experiments measuring μ [166,168,169,171,174]. For example, $\mu \approx 3.9$ for the network formed from PS particles [168], $\mu \approx 3.3$ for the network formed from silica particles [166], and $\mu \approx 4.2$ for the network formed from aqueous suspensions of Catapal and Dispal powders, the elastic properties of which have been found to correspond to the strong-link regime [174].

Up to now, we have considered systems for which the bonding energy is infinite, which means that a particle, once bound to its neighbours, can no longer escape, leading to an irreversible growth process which characterizes the gel formation. However, in many systems, the bonding energy between particles is not high enough to lead to this

irreversible growth process. This finite bonding energy induces a cluster fluid phase whose structure (fractal dimension and aggregation) depends on the value of the bonding energy, as we will see in the next section.

2.2.2. Reversible diffusion-limited colloidal aggregation (RDLC)

The effect of a finite bonding energy has been studied by introducing a finite inter-particle attraction energy - U into the irreversible DLCA simulation model. These simulations show that the breaking of the bonds allows the clusters to restructure and densify. These effects depend on the initial concentration of the system and concern both the fractal dimension of the particle clusters, which increases when the value of the bonding energy decreases [176], and their aggregation, for which several scenarios are possible depending on the value of the bonding energy [177]. When the bonding energy is high, but not high enough to lead to an irreversible growth process, the cluster growth remains fractal, but with a fractal dimension that increases due to the simultaneous compaction occurring on a small scale. The assembly of the clusters always presents the connected structure of a gel, but this structure does not fill all the space, unlike the gel. Therefore, this system is not a gel and it is actually a fluid of fractal elongated string-like clusters typical of DLCA. As the bonding energy decreases, the system gradually deviates from the gel structure, due to the compaction of clusters resulting from the finite bonding energy. The system is evolving towards a fluid of compact clusters on short-length scales but with a branched surface. When the density is low, a coarsening pattern of irregular and almost compact droplets is obtained. In summary, the finite bonding energy induces a cluster fluid phase whose structure depends on the value of the bond energy.

2.2.3. Jamming process

Jammed systems are another type of material that also has a solid-like response [178–187]. They refer to disordered systems, such as granular materials, foams, pastes, emulsions, and attractive colloidal suspensions, for which the thermal energy is insufficient to modify the packing of particles (athermal systems) [178–182]. They can flow when sheared, and jam when the shear stress is too low to induce a change in the packing of particles. These jammed materials resulting from crowding effects are, therefore, amorphous solids having yield stress like glasses have, with the difference that glasses are thermal systems obtained by lowering the temperature. Although the jamming and glass states have distinct physical origins, they share many similarities leading to the proposition of a unified jamming phase diagram for which thermal (glass materials) and athermal (jammed materials) systems belong to the same jammed phase diagram [178].

The jamming transition occurs when the concentration ϕ of the particles reaches a value for which the particles begin to touch each other. This transition has been studied for attractive systems with short-range interaction by studying their mechanical response at 0 K using numerical simulations [179,180]. The latter shows that the formation of the jammed systems is characterized by two transitions occurring when the concentration of the colloidal particles increases. The first transition is a second-order connectivity transition which corresponds to the transition from a non-percolated state (liquid-like) to a percolated but unjammed state (gel-like). This transition is followed by a second-order rigidity percolation transition which corresponds to the transition from the percolated state to the jammed state. These two transitions are distinct transitions with ϕ_P (connectivity percolation) $<$ ϕ_R (rigidity percolation). In summary, the formation of a jammed attractive colloidal system requires percolating clusters and a scenario with two critical transitions: first, a connectivity percolation and, then, a rigidity percolation. Therefore, the mechanism leading to the jammed state when the packing fraction increases is as follows: liquid \rightarrow connectivity percolation with force balance \rightarrow gel \rightarrow rigidity gel = jammed state.

In the case of repulsive colloidal systems, the connectivity transition between the non-percolated state and the percolated state - but

unjammed state - disappears, and the formation of the jammed state results simply from a first-order rigidity percolation transition.

The relationship between the amorphous jamming state (athermal system) and glass state (thermal system) has recently been studied by numerical simulations for a system composed of soft repulsive spheres [183,184]. These simulations show that the glass and the jammed system occur in two different regions, each characterized by different time scales and stress scales, which indicates that the jammed system and the glass system have distinct microscopic dynamics. As an illustration [181], the additivity of the contributions of the thermal and athermal components to the total shear stress shows that these domains can be well separated, e.g., hard colloidal micron-sized PMMA spheres controlled by glass physics [6–13] and aqueous foams controlled by jamming [185], or coexist, e.g., micron-sized emulsions [186]. Jamming only affects the low-temperature properties of the glassy phase [184], and appears as a change in the nature of the latter [187].

2.2.4. Cluster mode-coupling approach to weak gelation in attractive colloids

Although not based on the percolation model, this approach predicts that the quasi-irreversible bonding occurring in the low ϕ range of attractive colloidal suspensions can lead to a gel [188,189]. Actually, this approach is based on the mode coupling theory (MCT) for glasses, which provides a single framework to describe the structure of attractive colloidal systems for all ϕ . It consists in applying the MCT for two different scales: a short scale to the monomers, and a longer scale to the clusters (CMCT). The gelation process results from a two-stage ergodicity breaking that is linked to both the monomer scale and the cluster scale. The first ergodicity breaking occurs when the original suspension becomes kinetically unstable against aggregation, which leads to the formation of a fluid of coarse-grained clusters. The second ergodicity breaking occurs when the coarse-grained clusters stop growing and ϕ increases. This leads to an arrested state identified as a dense gel or an attractive glass. If the condition for the arrest is not met, the system is a cluster fluid.

3. Revisiting viscoelastic properties of colloidal systems with weakly attractive particles

Once the main mechanisms leading to the formation and mechanical properties of soft solids have been reviewed, the formation of three systems at low ϕ values with different attractive colloidal particles can be revisited, whose rheological properties have been studied in detail: suspensions of carbon black (CB) [24–27], suspensions of poly(methyl methacrylate) (PMMA) hard spheres with a depletion attraction induced by addition of polystyrene (PS) [26], and suspensions of amino acid organogelator molecules [28]. The solid-like behaviour observed in the systems has been interpreted as being due to a solid resulting from jamming of particles [25,26] and to a jammed suspension [28], respectively. We propose here another interpretation which shows that the solid-like response of all these systems corresponds to a change in the viscoelastic response of a cluster fluid occurring when the elastic component of the shear modulus G' becomes greater than the viscous component G'' .

3.1. Carbon black (CB) colloidal suspensions

These particles are attractive and transform the suspension into a network even when the concentration is very low. This attractive interaction can be precisely controlled by a dispersant agent which is absorbed as a surfactant on the surface of the CB particles. Trappe et al. [24,25] and Prasad et al. [26] reported the formation of a space-spanning network built from CB particles suspended in mineral oil as a function of the volume fraction ϕ of the particles ($0.056 < \phi < 0.149$) and the interparticle attractive interaction U ($5.2 < U/k_B T < 13.7$).

The CB suspension is described as composed of two independent

components, a solid network and a viscous fluid [24]. The formation of the solid network is governed by a power-law given by $G'_{\text{plateau}} \sim (\phi - \phi_c)^t$ with $t \approx 4$ and $\phi_c = 0.053$, and by a similar power-law for the variation of G'_{plateau} as a function of U with a value of $t \approx 4$. These power-law relations show that the formation of the solid network presents a critical behaviour resulting from a DLCA mechanism, with rigidity percolation as a possible origin of the exponent t . These observations could therefore suggest that the solid network is a gel. This assumption can be tested by considering the behaviour of G' and G'' as a function of frequency because a gel is characterized by $G' > G''$ for all frequencies. For the ϕ range studied, Fig. 1a (Fig. 1 in ref. [24]) shows that G' and G'' intersect, which leads to a solid-like response at the lowest frequencies ($G' > G''$) and a liquid-like response at the highest frequencies ($G'' > G'$). The intersection between G' and G'' indicates that the interactions between the CB particles are not strong enough to place the relaxation frequency beyond the experimental frequency range. The system is therefore not a gel. Since this DLCA mechanism does not lead to a gel, the natural way is to attribute the percolation mechanism to an RDLCA mechanism for which the bond energy is finite so that the growth process becomes reversible leading to relaxation effects. As recalled in Section 2.2.2, when the bonding energy is strong, but not strong enough to lead to irreversible growth, the cluster assembly has the connected structure of a gel. However, unlike the gel, this structure does not fill all the space and presents cluster growth which remains fractal with a fractal dimension value close to that of the DLCA or higher. The liquid-like behaviour could be explained by the removal of the weak inter-particle interactions ($1 < U/k_B T < 10$) at high shear frequencies. The crossover shift is directly proportional to the volume fraction of particles in the system, *i.e.*, the total number of interactions. At low ϕ , the total amount of interactions requires less energy to be removed than for high ϕ and, therefore, the crossover is shifted towards low-frequency values. Therefore, the particle system cannot hold the solid structure any longer becoming a liquid-like material. Moreover, when coming back to low frequencies or at rest, new and equivalent inter-particle interactions are formed and the solid-like structure is recovered leading again to the idea that the system is governed by an RDLCA mechanism. Thus, all these observations do not justify the presence of two independent components, *i.e.*, a solid network independent of a viscous liquid phase, and a cluster fluid could be proposed. This interpretation is compatible with the master curve shown in Fig. 1b (Fig. 2 in ref. [24]) since this master curve being based solely on scaling properties can reflect either the behaviour of a solid network immersed in a fluid or that of a cluster fluid which presents both an elastic contribution and a viscous contribution.

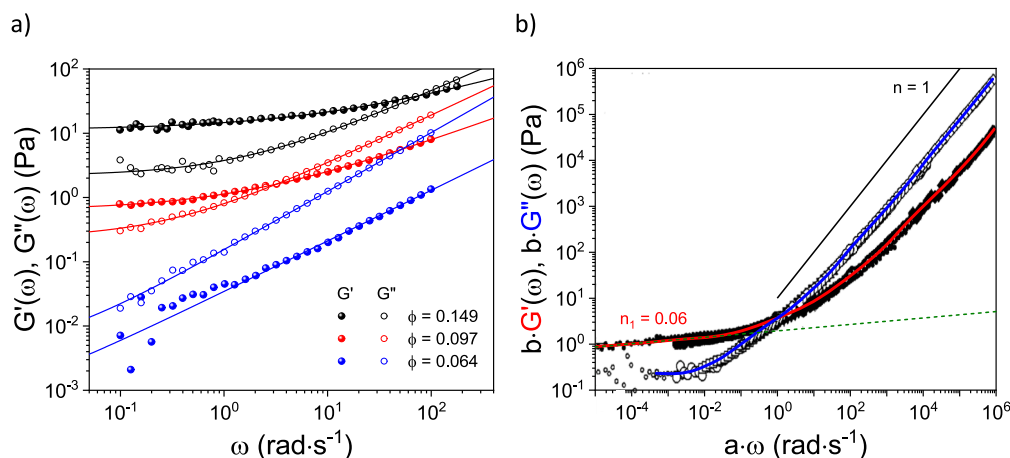


Fig. 1. (a) G' (filled symbols) and G'' (open symbols) frequency-sweep experiments for three different volume fractions of carbon black (CB) particles, *i.e.*, $\phi = 0.149$ (black), 0.097 (red), and 0.064 (blue), showing a solid-like and a liquid-like behaviour at low frequencies and high frequencies, respectively. Note that the crossover of $G' = G''$ is concentration-dependent. (b) Master curve showing the scaled moduli for different ϕ (open symbols) and U (solid symbols) as functions of the scaled frequency. The n_1 value corresponds to the slopes of G' at low frequencies obtained from adjustments based on power-law functions that serve as a guide to the eye. Plots adapted from ref. [24]. (For interpretation of the references to colour in this figure legend, the reader is referred to the web version of this article.)

It should be noted that this master curve shows that the elastic plateau characterizing the elastic response is never reached, suggesting again that the CB suspension is not a solid network for high ϕ or high U values, but rather a cluster fluid.

These observations lead us to propose that the solid-like response of the CB suspension for $0.056 < \phi < 0.149$ and $5.2 < U/k_B T < 13.7$ does not result from a fluid-to-solid transition, as claimed in ref. [23–25], but from a change in the viscoelastic response of the sol phase (cluster phase), which is characterized by the master curve of Fig. 1b (Fig. 2 in ref. [24]) and by an RDLCA mechanism of the rigidity type. On the other hand, the solid-like response of the system is not due to the jamming of clusters, because the formation of a jammed system requires a scenario with two critical transitions, connectivity and rigidity percolation (see Section 2.2.3), which are not observed here.

We close this chapter with the experiments carried out on CB suspensions as a function of temperature, from 25 °C to 100 °C, for a sample of 4.0 wt-% CB at a dispersant concentration of 1.0 wt-%. The master curve of Fig. 2 (Fig. 2 in ref. [27]) shows that this master curve perfectly

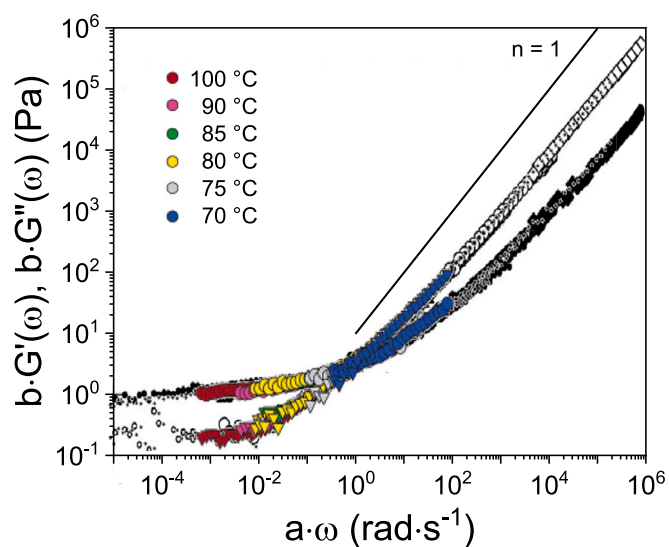


Fig. 2. Master curves for the two cluster fluids: CB as a function of ϕ (black symbols), and CB as a function of temperature (coloured symbols). Plots adapted from ref. [24] and [27].

superimposes on the master curves obtained as a function of CB concentration ϕ or interparticle interactions U . This demonstrates that the CB suspension as the temperature is varied is a cluster fluid and not a gel as claimed in ref. [27]. The interesting point is that the solid-like behaviour appears at high temperatures and the liquid-like behaviour at low temperatures, while the experiments carried out as a function of the concentration ϕ or as a function of the attractive interaction U showed that the liquid-like behaviour appears at low ϕ or low U values, and the solid-like behaviour at high ϕ or high U values. This means that the interaction energy varies with temperature so the effect of increasing temperature is the same as decreasing the strength of the attractive interaction, which comes from the increase in the concentration of the dispersant.

3.2. Colloidal suspension of hard spheres (PMMA) with depletion interaction

These systems are obtained by adding a non-adsorbing but dispersible polymer to a colloidal suspension of hard spheres, which leads to a depletion attraction - a concept introduced by Asakura et al. [17] and Vrij et al. [18] - between the colloidal particles when the polymer concentration is sufficient. The most studied system consists of PMMA hard spheres interacting only by volume exclusion and of a non-adsorbing PS random coil polymer - both dispersed in a simple hydrocarbon solvent as *cis*-decalin [19–21]. The exclusion of the polymer from the region between two neighbouring spheres causes an imbalance in the osmotic pressure, which pushes the spheres against each other, thus creating an effective depletion attraction between the spheres. The magnitude U of this attractive interaction is set by the concentration c_p of the polymer coil in the suspension and its range by the size ratio $\xi = r_g/R$ where r_g is the radius of gyration of the polymer coils and R is the radius of the colloidal particles. Therefore, the phase behaviour is controlled by both c_p and ξ , as well as by the colloidal volume fraction ϕ .

In the high-density regime, mode-coupling theories (MCT) [190–197], molecular dynamics (MD) simulations [21,198], and light scattering (LS) experiments [21] all show the existence of two distinct glassy states separated by a fluid: one is a repulsive glass where the arrest is due to caging by neighbouring particles, and the other is an attraction-dominated glass for which the particles are strongly bonded to each other due to high depletion attraction at higher depletion attraction. The existence of these two glassy states was confirmed by non-linear rheological measurements showing the presence of two yielding processes [198,199].

The low-density regime has also been the subject of numerous

experiments [26,132,200–204], in particular with confocal microscopy [201–204] and small-angle light scattering [200]. These experiments show the presence of a solid-like behaviour, interpreted as the CB suspension in the context of jamming transition.

Based on our analysis of the results on the carbon black suspensions, we re-analyzed the shear properties of the PMMA/PS suspensions studied in the low ϕ regime as a function of the three key parameters that characterize the system: the attractive interaction energy U , the volume fraction of particles ϕ and the size ratio ξ giving the range of the interaction [26]. The results obtained on PMMA/PS suspensions with large values of $U/k_B T = 13.7$ and 11.9 and a small value of $\xi \approx 0.04$, as well as those obtained on systems with small values of $U/k_B T = 7.1$ and 5.8 and a high value of $\xi \approx 0.18$, show that these systems have: (a) a frequency variation of G' and G'' at low $\phi \approx 0.1$ and low $U/k_B T$ (i.e., $U/k_B T = 3.6$ and $U/k_B T = 7.1$), very similar to that found for the carbon black suspension (Fig. 3a; Fig. 6 in ref. [26]), and (b) a master curve (Fig. 3b; Fig. 4 in ref. [26]) of the same shape as that obtained for the CB suspension with an elastic plateau that is never reached. This indicates that the elastic properties of these PMMA/PS suspensions are similar to those of the CB suspension and also to those of the suspension containing organogelator molecules, as will be shown in the next section.

Since the CB suspension is a cluster fluid with a cluster growth controlled by the RDLC mechanism, the same has to be true for the PMMA/PS suspensions quoted above. For the CB suspension, the RDLC mechanism is of the rigidity type ($t \approx 4$), but for the PMMA/PS suspensions, the critical exponent t depends on the range of interactions; $t \sim 2.1$ for long-range interactions ($\xi = 0.17$ and $U/k_B T = 7.1$ and 5.4) [26] and $t \sim 3.3$ for short-range interactions ($\xi = 0.04$ and $U/k_B T = 13.7$ and 11.9) [26].

In summary, PMMA/PS systems with large values of $U/k_B T$ and a small value of ξ or with small values of $U/k_B T$ and a high value of ξ , are cluster fluids arising from an RDLC mechanism based on rigidity percolation with a critical exponent that depends on the interaction range.

We will now compare the conclusion of our analysis of the results relating to these PMMA/PS suspensions, with experimental results obtained on other PMMA/PS suspensions.

Confocal microscopy studies [132,201–204] revealed the existence of stable cluster fluid for systems with small values of $U/k_B T$ and large values of ξ - e.g., $U/k_B T = 1.6$ and $\xi = 0.15$ [204], $U/k_B T = 5.1$ and $\xi = 0.11$ [202], and $U/k_B T = 4$ and $\xi = 0.15$ [132]. The fact that these cluster fluids are observed for low values of $U/k_B T$ and high values of ξ as in the case of the PMMA/PS suspensions [26] ($U/k_B T = 7.1$ and 5.8 with a high value of $\xi \approx 0.18$) confirms our analysis of the results from Prasad et al.

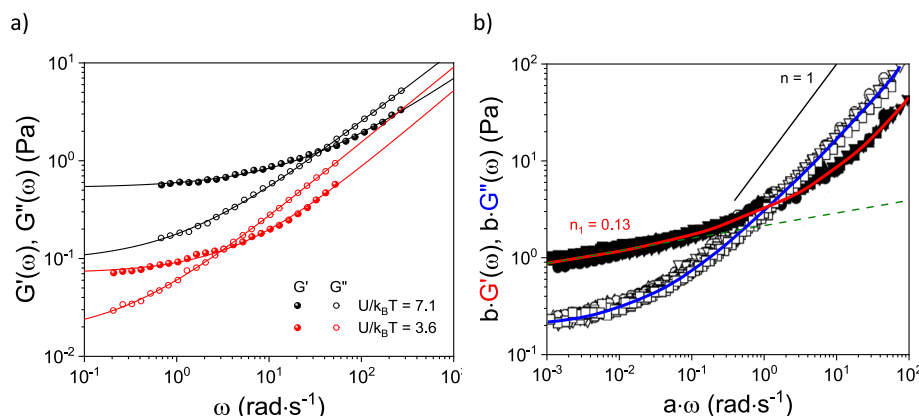


Fig. 3. (a) G' (filled symbols) and G'' (open symbols) frequency-sweep experiments at $\phi = 0.1$ for two different interaction values U for PMMA/PS systems, i.e., $U/k_B T = 7.1$ (black) and $U/k_B T = 3.6$ (red), showing a solid-like and a liquid-like behaviour at low frequencies and high frequencies, respectively. Note that the crossover of $G' = G''$ is energy-interaction dependent. (b) Master curve showing the scaled moduli obtained for different ϕ and ξ values as functions of the scaled frequency. The n_1 value corresponds to the slopes of G' at low frequencies obtained from adjustments based on power-law functions that serve as a guide to the eye. Plots adapted from ref. [26]. (For interpretation of the references to colour in this figure legend, the reader is referred to the web version of this article.)

[26] indicating that these systems are cluster fluids and not solid networks formed by the jamming of clusters.

On the other hand, the same studies showed the existence of a solid type structure - called gel by the authors - for the following systems: $U/k_B T = 12.2$ and $\xi = 0.11$ [202], $U/k_B T = 2.7$ and

$\xi = 0.11$ [204], and $U/k_B T = 4$ and $\xi = 0.19$ [132]. It should be noted that the systems of ref. [132, 204] have a low $U/k_B T$ value and a high value of ξ , which are characteristics of cluster fluids and not those of gels, as we saw previously. The assimilation of these systems to gels must therefore be taken with caution because it is not certain that the size (between 20 and 60 μm) of the image of the 2D confocal microscope is large enough to be sure that the system is a gel on the macroscopic scale. This question can be answered by rheological measurements. If a critical gel exists, the system is a gel and the cluster fluid is in the DLCA regime. If the critical gel does not exist, the system is not a gel and the cluster fluid corresponds to the RLCA regime, as we showed in the previous section dealing with carbon black suspensions. Such rheological experiments including critical gel measurements were made on some studies [14,15] but carried out on another type of system - dispersions of sticky hard spheres from octadecyl-coated silica particles - showing unambiguously that the system is a gel driven by a rigidity percolation from dilute ($\phi = 0.06$) to concentrate ($\phi = 0.52$) conditions [15].

Two final remarks to close this chapter. The first remark concerns the very low polymer density regime ($\phi = 2.2\%$) of the PMMA/PS system at $\xi \approx 0.08$, which was studied by confocal microscopy and small-angle light scattering [200,201]. The experiments were carried out at low colloidal concentrations and the strength between the colloidal particles was varied by the polymer concentration. Different regimes were observed depending on the polymer concentration and, therefore, the attractive force between the colloidal particles. By increasing the polymer concentration from zero, the authors successively observed a stable single-phase fluid (no phase separation), a phase separation *via* a nucleation-like mechanism, a phase separation *via* an aggregation mechanism producing compact clusters and an aggregation regime characterized by elongated clusters for the highest polymer concentration. In the first regime of aggregation, labelled as "RLCA", the clusters of particles are amorphous and rather compact, while in the second one, labelled as "DLCA", the amorphous clusters become ramified. This interesting evolution of the PMMA/PS system when the polymer concentration increases can be compared with the evolution of systems discussed in Section 2.2.2, for which the bonding energy increases progressively starting from a small value. This comparison strongly suggests that the RLCA regime observed for this PMMA/PS system is a cluster fluid.

The second remark concerns the experiments carried out on similar depletion-based systems, showing that gelation is driven by spinodal decomposition, a phase separation process driven by thermodynamic instability, leading to spanning clusters that arrest dynamically to form a gel [205,206]. This mechanism is suggested to apply to all hard sphere systems implying that gelation is a jamming transition induced by phase separation and not a homogeneous dynamical arrest within the fluid. However, the observation of a critical gel in the shear measurements carried out on suspensions of sticky hard spheres of octadecyl-coated silica particles [14,15] which lead to gels driven by rigidity percolation, shows that phase separation cannot be considered as the universal gelation mechanism as suggested in ref. [205, 206].

3.3. Suspensions of amino acid molecules leading to organogels

Organogels are systems described to date as physical gels formed by self-assembly in a suitable organic solvent of low molecular weight organic molecules called gelators [207]. A monograph on these systems has recently been written for those wishing to enter this field [208]. Unfortunately, this book has many inconsistencies, misconceptions and misrepresentations, and we simply wish to point out some of them that would lead new researchers in this field to the wrong research direction.

Several typical examples are: a) the organogel is considered as a gel and the author reproduces for the organogels the erroneous information which he provided for the gels throughout the book, e.g., organogels result from a first-order transition and that the temperature of the sol-organogel transition is detected by DSC measurements, which questions the validity of some of the phase diagrams of the book; b) the rheological content is reduced to the strict minimum, in particular, no mention is made of the critical gel that determines whether or not the soft solid studied is a gel allowing to the rigorous determination of the gel point; and c) the author indicates that the critical gel concentration c_{gel} is not a critical parameter unlike the critical bond probability p_c , and that the study of rheological properties as a function of $(c - c_{\text{gel}})/c_{\text{gel}}$ is therefore irrelevant. Clearly, the author seems to ignore the literature on colloidal gels showing that c_{gel} is a critical parameter and that the formation of DLCA gels is expressed as a function of $(c - c_{\text{gel}})/c_{\text{gel}}$.

The amino acid (AA) organogels can be considered as the prototype of organogels formed by clusters of rod-like particles. Their mechanical properties have recently been studied as a function of both the temperature - for several selected clusters' volume fraction ϕ values - and of a cluster's volume fraction - at a given temperature [28]. The central point of this study is to show that the organogel is not a physical gel contrary to the current belief, because G' and G'' intersect in the state where G' has a solid-like response.

The organogelator molecule used to form the toluene-based and the tetralin-based organogel is a peptide protected by a benzyloxycarbonyl (Z) group and by a hydrazine naphthalimide (NH-Napht.) group at its *N*-terminal at its *C*-terminal end, respectively. The structure of the network was determined by X-ray experiments performed on the organogelator molecule - pristine sample - after the synthesis (Fig. SI-1 and SI-2). The results indicate that the network is formed by randomly distributed fibres constituted by a bundle of fibrils. The internal fibre structure follows a hexagonal packing of the fibrils, which interact by π - π stacking along the fibre axis. Each single fibril results from the self-organization of the organogelator molecule in a uniaxial fashion controlled by hydrogen bonds between the amino acid moieties. These observations indicate that the semi-flexible fibres are constituted from long-packed fibrils and, therefore, that the resulting network is formed when fibres interact in all directions in a disordered fashion. The concentration range in organogelator molecules was between 0.2 % and 7 % and the experiments were performed in the linear response regime as those of the CB and the PMMA/PS systems.

The experiments carried out as a function of temperature for a given concentration of organogelator molecules show that the mechanical response of the solution presents three different regions characterized by three different rheological behaviours occurring by decreasing the temperature: a liquid region associated with the free organogelator molecules (region I), a liquid-type region (region II) associated with the formation of clusters resulting from the association of organogelator molecules, and a solid-type region (region III) characterizing the organogel. The transition temperature, $T_{\text{organogel}}$ between the cluster fluid and the organogel corresponds to the crossing of G' and G'' . The value of $T_{\text{organogel}}$ depends on the cooling rate, the frequency used during the measurements and the concentration of organogelator molecules - a typical sequence is given by Fig. 4, 5, 6, and 7 in ref. [28] relating to a solution based on tetralin at 0.2 %. It should be noted that the suspension of organogel molecules is more documented than the other suspensions studied in this paper, because it shows the different steps leading to the formation of the solid-like state.

The G' and G'' measurements carried out at temperatures around $T_{\text{organogel}}$ - the temperature at which a solid is formed ($G' > G''$) upon cooling - show that the critical gel characterized by the relationship $G' \sim G'' \sim \omega^n$ is not observed (Fig. 4a; Fig. 9 in ref. [28]). This indicates that percolation is not the mechanism for the formation of the organogel. As a result, the liquid-solid transition is not a sol-gel transition, and, therefore, the organogel is not a physical gel.

The results obtained for a given concentration of organogel

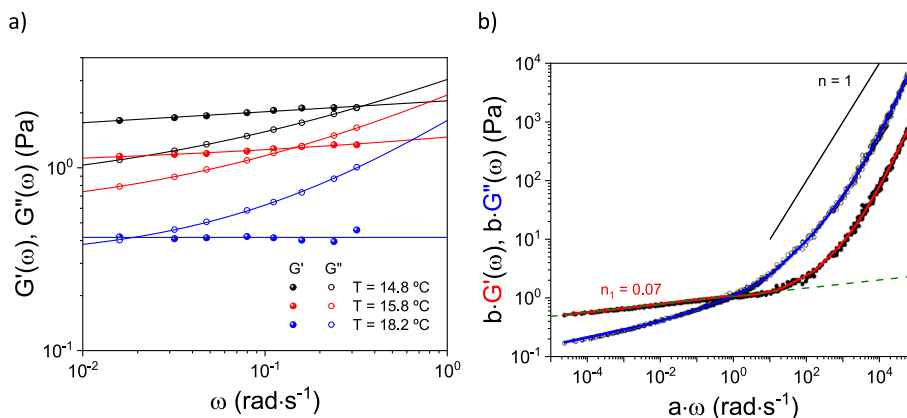


Fig. 4. (a) G' (filled symbols) and G'' (open symbols) frequency-sweep experiments at $C = 0.2\%$ at different temperatures located around the transition temperature $T = 15.8\text{ }^{\circ}\text{C}$ for the AA organogelator molecule, *i.e.*, $T = 18.2\text{ }^{\circ}\text{C}$ (blue), $15.8\text{ }^{\circ}\text{C}$ (red) and $14.8\text{ }^{\circ}\text{C}$ (black) -, showing a solid-like and a liquid-like behaviour at low frequencies and high frequencies, respectively. Note that the crossover of $G' = G''$ is temperature-dependent. (b) Master curve showing the scaled moduli for different temperatures as functions of the scaled frequency. The n_1 value corresponds to the slopes of G' at low frequencies obtained from adjustments based on power-law functions that serve as a guide to the eye. Plots adapted from ref. [28]. (For interpretation of the references to colour in this figure legend, the reader is referred to the web version of this article.)

molecules as a function of temperature for temperatures below $T_{\text{organogel}}$ (Fig. 17 in ref. [28]), and those obtained as a function of the concentration C for a given temperature belonging to the solid type region characterizing the organogel (Fig. 14 in ref. [28]) show a critical type behaviour of the elastic plateau G'_p with a critical exponent $\nu_c \approx 2$. The analysis of G' as a function of temperature for a given concentration gives a value slightly higher than $T_{\text{organogel}}$ - for the solid formation temperature T^* -, which is not surprising given that $T_{\text{organogel}}$ is associated with the behaviour of the solution and not of the solid. Values of the critical exponent $\nu_c = 2.1$ and 3.3 have been reported for PMMA/PS suspensions (see Section 3.2) and interpreted in the context of rigidity percolation which predicts a value of $\nu_c \approx 2.1$ for bonds resistant to stretching formed by long-range attractive interactions between the clusters [101], and a value of $\nu_c \approx 3.75$ for bonds resistant to both stretching and bending for short-range interactions [52]. Our value of $\nu_c \approx 2$ suggests that the organogel has bonds that resist stretching but not bending. However, the absence of a critical gel prevents us from assimilating the organogel to a physical gel associated with a DLCA mechanism of the rigidity type. It is rather a fluid of clusters resulting from an RDLCAs aggregation associated with a rigidity-like mechanism.

As for the CB suspension and the PMMA/PS systems, the viscoelastic properties of the organogelator suspension can be summarized by a master curve (Fig. 4b; Fig. 19 in ref. [28]), the shape of which is similar to that of the CB and PMMA/PS suspensions, with an elastic plateau never reached. This master curve was constructed in the same way as that obtained previously for the CB suspension by choosing as a reference the data of G' and G'' taken at a temperature for which the variations of both moduli as a function of temperature intersect at a well-determined frequency (Fig. 4b; Fig. 19 in ref. [28]). The other curves were shifted along the frequency axis (scale factor a) and the module axis (scale factor b). The result, therefore, represents the viscoelastic response of the system for this temperature and this reference frequency. Above the crossing temperature, G'' is greater than G' , so that the system behaves like a liquid. Below the crossing temperature, G' is larger than G'' , so that the system behaves like a solid. The crossing temperature is, therefore, not a transition temperature between two states. It is a temperature that is associated with a modification of the response of the suspension, its elastic contribution becoming greater than its viscous contribution. In other words, the organogelator suspension is a cluster fluid. The dashed line in Fig. 4b confirms that the solid-like response of the organogel begins above the crossover temperature.

As can be seen, these rheological experiments give very similar results to those obtained on the CB suspensions and the PMMA/PS

systems, showing that the solid-like response of these systems does not come from a fluid-to-solid transition associated with jamming but from a change in the viscoelastic response of the liquid phase formed by the clusters, the so-called cluster fluid, which is characterized by master curves of the same shape and by a rigidity-type RDLCAs mechanism. Finally, it should be noted that static compression experiments carried out on the suspension of organogelator molecules in the solid-type region show a thixotropic behaviour when the space between the two sample-bearing glass slides of the rheometer cell is reduced, instead of the elastic response expected for a gel or a solid (Fig. 15 in ref. [28]), therefore, confirming the fluid nature of the system.

A more detailed comparison between the three cluster fluids was carried out by superimposing the corresponding master curves, plotting all storage G' and loss G'' moduli at the $a \cdot \omega = 1$ (Fig. 5). The result indicates that both isotropic CB particles (black symbols) and PMMA hard spheres (red symbols) match quite well for both the G' (full symbols) and

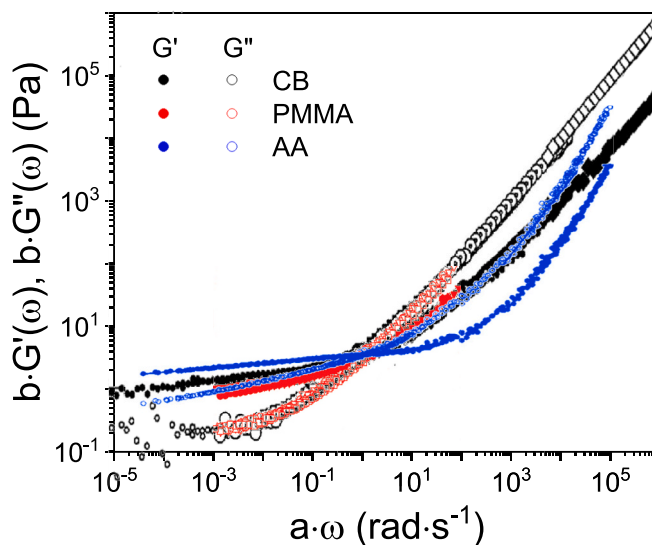


Fig. 5. Master curves for the three clusters fluids: CB (black), PMMA (red) and AA (blue) showing that the master curve of the rod-like organogelator particles does not match the master curve of isotropic CB particles and hard spheres PMMA particles with depletion interaction. (For interpretation of the references to colour in this figure legend, the reader is referred to the web version of this article.)

Gⁿ (empty symbols) behaviour, while the anisotropic AA organogelator rod-like particles (blue symbols) do not match at all. It appears that anisotropy and, consequently, connectivity and interaction between particles, have a direct effect on the rheological behaviour of such systems.

4. Conclusion

In this manuscript, firstly, a short overview of the different concepts, *i.e.*, gelation, aggregation, jamming, cluster mode-coupling approach, has been presented with the purpose of describing the transition between a liquid and a solid, with a particular focus on the models of critical gel, irreversible diffusion-limited colloidal aggregation (DLCA), reversible diffusion-limited colloidal aggregation (RDLC), and reaction-limited colloidal aggregation (RLCA) processes. These models have made it possible to describe, rheologically, the liquid-to-solid transition of different systems made up of attractive particles at low concentrations, which are the subject of the second part of the manuscript.

Secondly, the manuscript revisited in detail three different colloidal systems, *i.e.*, carbon black (CB) suspensions, poly(methyl methacrylate)/polystyrene (PMMA/PS) suspensions, and suspensions of amino acid (AA) organogelator molecules giving rise to the organogel, for which rheological measurements have been carried out.

Our analysis shows that CB suspensions, suspensions of AA molecules, as well as PMMA/PS suspensions with large values of $U/k_B T$ and a small value of ξ , or *vice-versa*, are not solid phases resulting from a fluid to solid transition supporting the jamming concept. These are cluster fluids arising from an RDLC mechanism based on rigidity percolation with a critical exponent depending on the interaction range, whose viscoelastic properties are described by master curves of the same shape. The temperature of the liquid-to-solid transition is, therefore, not a transition temperature between a liquid and a solid state, but a temperature reflecting a change in the response of the suspension, when the elastic contribution becomes more important than the viscous contribution. Of course, this behaviour change is a function of frequency, cooling rate and concentration. Since many colloidal systems at low concentrations of weakly attractive solid particles are not gels but cluster fluids, the analysis of their data should be reconsidered.

Although the colloidal systems that we reanalyzed are cluster fluids, it should be noted that gels driven by rigidity percolation have been unambiguously observed [15] in the case of suspensions of sticky hard spheres, for which the existence of the gel was established by the observation of a critical gel [13,14], and the rigidity percolation by the coordination number $\langle N_b \rangle$ which is equal to 2.4, as for mean-field transitions in random networks (see Section 2.1.2.1). As noted in ref. [15], the observation of a gel driven by rigidity percolation indicates that the phase separation observed on several depletion-based systems cannot be considered as the universal gelation mechanism for all the attractive hard sphere systems, as suggested in ref. [205].

CRedit authorship contribution statement

Philippe Martinoty: Conceptualization, Methodology, Investigation, Writing - Original Draft, Writing - review & editing. **Antoni Sánchez-Ferrer:** Software, Formal analysis, Investigation, Writing - review & editing, Visualization.

Declaration of competing interest

The authors declare that they have no known competing financial interests or personal relationships that could have appeared to influence the work reported in this paper.

Data availability

Data will be made available on request.

Acknowledgements

We thank Veronique Trappe (Physics Department, University of Fribourg, Switzerland) for discussions on jamming.

Appendix A. Supplementary data

Supplementary data to this article can be found online at <https://doi.org/10.1016/j.cis.2024.103335>.

References

- [1] de Gennes PG. *Scaling concepts in polymers physics*. Cornell University Press; 1979. ISBN: 080141203X.
- [2] Rubinstein M, Colby RH. *Polymer physics*. Oxford University Press; 2003. ISBN: 019852059X.
- [3] Stauffer D, Coniglio A, Adam M. Gelation and critical phenomena. *Adv Polym Sci* 1982;44:103–58. https://doi.org/10.1007/3-540-11471-8_4.
- [4] Stauffer D. *Introduction to percolation theory*. Francis & Taylor; 1985. ISBN: 0850663156.
- [5] Adam M, Lairez D. *The physical properties of polymer gels*. John Wiley and Sons; 1996. ISBN: 0471939714.
- [6] Nijenhuis K. *Thermoreversible networks: viscoelastic properties and structure of gels*. Springer-Verlag; 1997. <https://doi.org/10.1007/BFb0008699>.
- [7] Pusey PN, van Meegen W. Phase behaviour of concentrated suspensions of nearly hard colloidal spheres. *Nature* 1986;320:340–2. <https://doi.org/10.1038/320340a0>.
- [8] Pusey PN, van Meegen W. Observation of a glass transition in suspensions of spherical colloidal particles. *Phys Rev Lett* 1987;59:2083–6. <https://doi.org/10.1103/PhysRevLett.59.2083>.
- [9] Rouw PW, de Kruijff CG. Adhesive hard-sphere colloidal dispersions: fractal structures and fractal growth in silica dispersions. *Phys Rev A* 1989;39:5399–408. <https://doi.org/10.1103/PhysRevA.39.5399>.
- [10] Chen M, Russel WB. Characteristics of flocculated silica dispersions. *J Colloid Interface Sci* 1991;141:564–77. [https://doi.org/10.1016/0021-9797\(91\)90353-A](https://doi.org/10.1016/0021-9797(91)90353-A).
- [11] Grant MC, Russel WB. Volume-fraction dependence of elastic moduli and transition temperatures for colloidal silica gels. *Phys Rev E* 1993;47:2606–14. <https://doi.org/10.1103/PhysRevE.47.2606>.
- [12] Negi AS, Redmon CG, Ramakrishnan S, Osuji CO. Viscoelasticity colloidal gel during dynamical arrest. *J Rheol* 2014;58:1557–615. <https://doi.org/10.1122/1.4883675>.
- [13] Eberle APR, Wagner NJ, Castañeda-Priego R. Dynamical arrest transition in nanoparticle dispersions with short-range interactions. *Phys Rev Lett* 2011;106:105704. <https://doi.org/10.1103/PhysRevLett.106.105704>.
- [14] Eberle APR, Castañeda-Priego R, Kim JM, Wagner NJ. Dynamical arrest, percolation, gelation, and glass formation in model nanoparticle dispersions with Thermoreversible adhesive interactions. *Langmuir* 2012;28:1866–78. <https://doi.org/10.1021/la2035054>.
- [15] Valadez-Perez NE, Liu Y, Eberle APR, Wagner NJ, Castañeda-Priego R. Dynamical arrest in adhesive hard-sphere dispersions driven by rigidity percolation. *Phys Rev E* 2013;88. <https://doi.org/10.1103/PhysRevE.88.060302>. 060302(R).
- [16] Kim JM, Fang J, Eberle APR, Castañeda-Priego R, Wagner NJ. Gel transition in adhesive hard-sphere colloidal dispersions: the role of gravitational effects. *Phys Rev Lett* 2013;110:208302. <https://doi.org/10.1103/PhysRevLett.110.208302>.
- [17] Asakura S, Oosawa F. On interaction between two bodies immersed in a solution of macromolecules. *J Chem Phys* 1954;22:1255–6. <https://doi.org/10.1063/1.1740347>.
- [18] Vrij A. Polymers at interfaces and the interactions in colloidal dispersions. *Pure Appl Chem* 1976;48:471–83. <https://doi.org/10.1351/pac197648040471>.
- [19] Poon WCK. The physics of a model colloid-polymer mixture. *J Phys Condens Matter* 2002;14:R859–80. <https://doi.org/10.1088/0953-8984/14/33/201>.
- [20] Poon WCK. Colloidal glasses. *MRS Bull* 2004;29:96–9. <https://doi.org/10.1557/mrs2004.35>.
- [21] Pham KN, Puertas AM, Bergholtz J, Egelhaaf SU, Moussaid A, Pusey PN, et al. Multiple glassy states in a simple model system. *Science* 2002;296:104–6. <https://doi.org/10.1126/science.1068238>.
- [22] Trappe V, Sandkühler P. Colloidal gels-low density disordered solid-like states. *Curr Opin Colloid Interface Sci* 2004;8:494–500. <https://doi.org/10.1016/j.cocis.2004.01.002>.
- [23] Zaccarelli E. Colloidal gels: equilibrium and non-equilibrium routes. *J Phys Condens Matter* 2007;19:323101. <https://doi.org/10.1088/0953-8984/19/32/323101>.
- [24] Trappe V, Weitz DA. Scaling of the viscoelasticity of weakly attractive particles. *Phys Rev Lett* 2000;85:449–52. <https://doi.org/10.1103/PhysRevLett.85.449>.
- [25] Trappe V, Prasad V, Cipolletti L, Segre P, Weitz DA. Jamming phase diagram for attractive particles. *Nature* 2001;411:772–5. <https://doi.org/10.1038/35081021>.

- [26] Prasad V, Trappe V, Dinsmore A, Segre P, Cipelletti L, Weitz DA. Universal features of the fluid to solid transition for attractive colloidal particles. *Faraday Discuss* 2003;123:1–12. <https://doi.org/10.1039/B211107C>.
- [27] Won YY, Meeker S, Trappe V, Weitz DA, Diggs NZ, Emert JI. Effect of temperature on carbon-black agglomeration in hydrocarbon liquid with adsorbed dispersant. *Langmuir* 2005;21:924–32. <https://doi.org/10.1021/la047906t>.
- [28] Collin D, Covis R, Allix F, Jamart-Gregoire B, Martinoty P. Jamming transition in solutions containing Organogelator molecules of amino-acid type: rheological and calorimetry experiments. *Soft Matter* 2013;9:2947–58. <https://doi.org/10.1039/C2SM26091C>.
- [29] Chen DTN, Wen Q, Janmey PA, Crocker JC, Yodh AG. Rheology of soft materials. *Annu Rev Condens Matter Phys* 2010;1:301–2. <https://doi.org/10.1146/annurev-conmatphys-070909-104120>.
- [30] Martinoty P. Selected mechanical properties of uniaxial side chain liquid crystalline elastomers. In: *Liquid Crystalline Polymers*. Springer; 2015. https://doi.org/10.1007/978-3-319-20270-9_3.
- [31] Rogez D, Krause S, Martinoty P. Main-chain liquid-crystal elastomers versus side-chain liquid-crystal elastomers: similarities and differences in their mechanical properties. *Soft Matter* 2018;14:6449–62. <https://doi.org/10.1039/C8SM00936H>.
- [32] Chambon F, Winter HH. Analysis of linear viscoelasticity of a crosslinking polymer at the gel point. *J Rheol* 1986;30:367–82. <https://doi.org/10.1122/1.549853>.
- [33] Chambon F, Winter HH. Linear viscoelasticity at the gel point of a crosslinking PDMS with imbalanced stoichiometry. *J Rheol* 1987;31:683–97. <https://doi.org/10.1122/1.549955>.
- [34] Haan SW, Zwanzig R. Series expansions in a continuum percolation problem. *J Phys A* 1977;10:1547–55. <https://doi.org/10.1088/0305-4470/10/9/013>.
- [35] Vicsek T, Kertesz J. Monte Carlo renormalisation-group approach to percolation on a continuum: test of universality. *J Phys A* 1981;14:L31–7. <https://doi.org/10.1088/0305-4470/14/2/003>.
- [36] Gawlinsky ET, Stanley HE. Continuum percolation in two dimensions: Monte Carlo tests of scaling and universality for non-interacting discs. *J Phys A* 1981;14:L291–9. <https://doi.org/10.1088/0305-4470/14/8/007>.
- [37] Flory PJ. Molecular size Distribution in three dimensional polymers. I - gelation. *J Am Chem Soc* 1941;63:3083–90. <https://doi.org/10.1021/ja01856a061>.
- [38] Flory PJ. Molecular size Distribution in three dimensional polymers. II - trifunctional branching units. *J Am Chem Soc* 1941;63:3091–6. <https://doi.org/10.1021/ja01856a062>.
- [39] Stockmayer WH. Theory of molecular size Distribution and gel formation in branched-chain polymers. *J Chem Phys* 1943;11:45–55. <https://doi.org/10.1063/1.1723803>.
- [40] Stockmayer WH. Theory of molecular size Distribution and gel formation in branched polymers II. General cross-linking. *J Chem Phys* 1944;12:125–31. <https://doi.org/10.1063/1.1723922>.
- [41] Stauffer D. Gelation in concentrated critically branched polymer solutions. Percolation scaling theory of intramolecular bond cycles. *J Chem Soc Faraday Trans* 1976;2(72):1354–64. <https://doi.org/10.1039/F29767201354>.
- [42] de Gennes PG. On a relation between percolation theory and the elasticity of gels. *J Physique Lett* 1976;37:L1–2. <https://doi.org/10.1051/jphyslet:019760037010100>.
- [43] de Gennes PG. Incoherent scattering near a sol-gel transition. *J Physique Lett* 1979;40:L197–9. <https://doi.org/10.1051/jphyslet:01979004009019700>.
- [44] Allain C, Salome L. Sol-gel transition of hydrolyzed polyacrylamide + chromium (III). Rheological behavior versus cross-link concentration. *Macromolecules* 1987;20:2957–8. <https://doi.org/10.1021/ma00177a056>.
- [45] Martin JE, Adolf D, Wilcoxon JP. Viscoelasticity of near-critical gels. *Phys Rev Lett* 1988;61:2620–3. <https://doi.org/10.1103/PhysRevLett.61.2620>.
- [46] Martin JE, Adolf D, Wilcoxon JP. Viscoelasticity near the sol-gel transition. *Phys Rev A* 1989;39:1325–32. <https://doi.org/10.1103/PhysRevA.39.1325>.
- [47] Herrmann HJ, Stauffer D. Phase diagram for three-dimensional correlated site-bond percolation. *Z Phys B Condensed Matter* 1981;44:339–44. <https://doi.org/10.1007/BF01294172>.
- [48] Muthukumar M. Screening effect on viscoelasticity near the gel point. *Macromolecules* 1989;22:4656–8. <https://doi.org/10.1021/ma00202a050>.
- [49] Derrida B, Stauffer D, Herrmann HJ, Vannimenus J. Transfer matrix calculation of conductivity in three-dimensional random resistor networks at percolation threshold. *J Physique Lett* 1983;44:L701–6. <https://doi.org/10.1051/jphyslet:019830044017070100>.
- [50] Herrmann HJ, Derrida B, Vannimenus J. Superconductivity exponents in two and three-dimensional percolation. *Phys Rev B* 1984;30:4080–2. <https://doi.org/10.1103/PhysRevB.30.4080>.
- [51] Zabolitzky JG. Monte Carlo evidence against the Alexander-Orbach conjecture for percolation conductivity. *Phys Rev B* 1984;30:4077–9. <https://doi.org/10.1103/PhysRevB.30.4077>.
- [52] Sahimi M, Arbabi S. Mechanics of disordered solids. II - Percolation on elastic networks with bond-bending forces. *Phys Rev B* 1993;47:703–12. <https://doi.org/10.1103/PhysRevB.47.703>.
- [53] Sahimi M, Goddard JD. Superelastic percolation networks and the viscosity of gels. *Phys Rev B* 1985;32:1869–71. <https://doi.org/10.1103/PhysRevB.32.1869>.
- [54] Alexander S. Is the elastic energy of amorphous materials rotationally invariant? *J Phys France* 1984;45:1939–45. <https://doi.org/10.1051/jphys:0198400450120193900>.
- [55] Yu KW, Chaikin PM, Orbach R. Relationship between the bulk modulus and the conductivity on a fractal. *Phys Rev B* 1983;28:4831–2. <https://doi.org/10.1103/PhysRevB.28.4831>.
- [56] Adolf D, Martin JE, Wilcoxon JP. Evolution of structure and viscoelasticity in an epoxy near the sol-gel transition. *Macromolecules* 1990;23:527–31. <https://doi.org/10.1021/ma00204a028>.
- [57] Matejka L. Rheology of epoxy networks near the gel point. *Polym Bull* 1991;26:109–16. <https://doi.org/10.1007/BF00299355>.
- [58] Eloundou JP, Feve M, Gerard JF, Harran D, Pascault JP. Temperature dependence of the behavior of an epoxy-amine system near the gel point through viscoelastic study. 1. Low-Tg epoxy-amine system. *Macromolecules* 1996;29:6907–16. <https://doi.org/10.1021/ma960287d>.
- [59] Eloundou JP, Gerard JF, Harran D, Pascault JP. Temperature dependence of the behavior of a reactive epoxy-amine system by means of dynamic rheology. 2. High-Tg epoxy-amine system. *Macromolecules* 1996;29:6917–27. <https://doi.org/10.1021/ma9602886>.
- [60] Mortimer S, Ryan AJ, Stanford JL. Rheological behavior and gel-point determination for a model Lewis acid-initiated chain growth epoxy resin. *Macromolecules* 2001;34:2973–80. <https://doi.org/10.1021/ma01835x>.
- [61] Adolf D, Martin JE. Time-cure superposition during crosslinking. *Macromolecules* 1990;23:3700–4. <https://doi.org/10.1021/ma00217a026>.
- [62] Trappe V, Richtering V, Burchard V. Critical behavior of anhydride cured epoxies. *J Phys II France* 1992;2:1453–63. <https://doi.org/10.1051/jp2:1992212>.
- [63] Chambon F, Petrovic ZS, MacKnight WJ, Winter HH. Rheology of model polyurethanes at the gel point. *Macromolecules* 1986;19:2146–9. <https://doi.org/10.1021/ma00162a007>.
- [64] Winter H, Morganeli P, Chambon R. Stoichiometry effects on rheology of model polyurethanes at the gel point. *Macromolecules* 1988;21:532–5. <https://doi.org/10.1021/ma00180a048>.
- [65] Durand D, Delsanti M, Adam M, Luck JM. Frequency dependence of viscoelastic properties of branched polymers near gelation threshold. *Europhys Lett* 1987;3:297–301. <https://doi.org/10.1209/0295-5075/3/3/008>.
- [66] Izuka A, Winter HH, Hashimoto T. Temperature dependence of viscoelasticity of polycaprolactone critical gels. *Macromolecules* 1994;27:6883–8. <https://doi.org/10.1021/ma00101a028>.
- [67] Antonietti M, Folsch KJ, Sillescu H, Pakula T. Micronetworks by end-linking of polystyrene. 2. Dynamic mechanical behavior and diffusion experiments in the bulk. *Macromolecules* 1989;22:2812–7. <https://doi.org/10.1021/ma00196a047>.
- [68] Scalán JC, Winter HH. Composition dependence of the viscoelasticity of end-linked poly(dimethylsiloxane) at the gel point. *Macromolecules* 1991;24:47–54. <https://doi.org/10.1021/ma00001a008>.
- [69] de Rosa ME, Mours M, Winter HH. The gel point as reference state: a simple kinetic model for crosslinking polybutadiene via Hydroxylation. *Polym Gels Nets* 1997;1997(5):69–94. [https://doi.org/10.1016/S0966-7822\(96\)00033-0](https://doi.org/10.1016/S0966-7822(96)00033-0).
- [70] Lusignea CP, Mourey T, Wilson JC, Colby RH. Viscoelasticity of randomly branched polymers in the critical percolation class. *Phys Rev E* 1995;52:6271–80. <https://doi.org/10.1103/PhysRevE.52.6271>.
- [71] Colby RH, Gillmor JR, Rubinstein M. Dynamics of near-critical polymer gels. *Phys Rev E* 1993;48:3712–6. <https://doi.org/10.1103/PhysRevE.48.3712>.
- [72] Takahashi M, Yokoyama K, Masuda T, Takigawa T. Dynamic viscoelasticity and critical exponents in sol-gel transition of an end-linking polymer. *J Chem Phys* 1994;101:798–804. <https://doi.org/10.1063/1.468135>.
- [73] Isaacson J, Lubensky TC. Flory exponents for generalized polymer problems. *J Phys Lett* 1980;41:469–71. <https://doi.org/10.1051/jphyslet:019800041019046900>.
- [74] de Gennes PG. Amas sur des réseaux: sur la différence entre la percolation et la statistique des "animaux". *Comptes Rend Acad Sci Paris* 1980;291:17.
- [75] Brown E, Essam JW, Place CM. Critical temperature of the Heisenberg model with random bond dilution. *J Phys C* 1975;8:321335. <https://doi.org/10.1088/0022-3719/8/3/011>.
- [76] Agrawal P, Redner S, Reynolds PJ, Stanley HE. Site-bond percolation: a low-density series study of the uncorrelated limit. *J Phys A* 1979;12:2073–85. <https://doi.org/10.1088/0305-4470/12/11/018>.
- [77] Nakanishi H, Reynolds PJ. Site-bond percolation by position-space renormalization group. *Phys Lett* 1979;71A:252–4. [https://doi.org/10.1016/0375-9601\(79\)90178-6](https://doi.org/10.1016/0375-9601(79)90178-6).
- [78] Hoshen J, Klymko P, Kopelman R. Percolation and cluster distribution. III. Algorithms for the site-bond problem. *J Stat Phys* 1979;21:583–600. <https://doi.org/10.1007/BF01011170>.
- [79] Daoud M, Leibler L. Randomly branched polymers: semi-dilute solutions. *Macromolecules* 1988;21:1497–501. <https://doi.org/10.1021/ma00183a045>.
- [80] Martin JE, Adolf D, Odineck J. Relaxation phenomena near the sol-gel transition. *Makromol Chem Makromol Symp* 1990;40:1–21. <https://doi.org/10.1002/masy.19900400104>.
- [81] Hodgson DF, Amis EJ. Dynamic viscoelastic characterization of sol-gel reactions. *Macromolecules* 1990;23:2512–9. <https://doi.org/10.1021/ma00211a019>.
- [82] Hodgson DF, Amis EJ. Dynamic viscoelasticity during a sol-gel reaction. *Phys Rev A* 1990;41:1182–5. <https://doi.org/10.1103/PhysRevA.41.1182>.
- [83] Martin JE, Wilcoxon JP, Schaeffer DW, Odineck J. Fast aggregation of colloidal silica. *Phys Rev A* 1990;41:4379–91. <https://doi.org/10.1103/PhysRevA.41.4379>.
- [84] Martin JE. Slow aggregation of colloidal silica. *Phys Rev A* 1987;36:3415–26. <https://doi.org/10.1103/PhysRevA.36.3415>.
- [85] te Nijenhuis K, Winter HH. Mechanical properties at the gel point of a crystallizing poly(vinyl chloride) solution. *Macromolecules* 1989;22:411–4. <https://doi.org/10.1021/ma00191a074>.

- [86] Li L, Aoki Y. Rheological images of poly(vinyl chloride) gels. 1. The dependence of sol-gel transition on concentration. *Macromolecules* 1997;30:7835–41. <https://doi.org/10.1021/ma971045w>.
- [87] Aoki Y, Li L, Uchida H, Kakiuchi M, Watanabe H. Rheological images of poly(vinyl chloride) gels. 5. Effect of molecular weight Distribution. *Macromolecules* 1998;31:7472–8. <https://doi.org/10.1021/ma971889f>.
- [88] Aoki Y, Li L, Kakiuchi M. Rheological images of poly(vinyl chloride) gels. 6. Effect of temperature. *Macromolecules* 1998;31:8117–23. <https://doi.org/10.1021/ma980556v>.
- [89] Miyoshi E, Nishinari K. Rheological and thermal properties near the sol-gel transition of Gellan gum aqueous solutions. *Progr Colloid Polymer Sci* 1999;114:68–82. https://doi.org/10.1007/3-540-48349-7_11.
- [90] Sato T, Watanabe H, Osaki K. Thermoreversible physical gelation of block copolymers in a selective solvent. *Macromolecules* 2000;33:1686–91. <https://doi.org/10.1021/ma991602+>.
- [91] Fuchs T, Richtering W, Burchard W, Kajiwara K, Kitamura S. Gel point in physical gels rheology and light scattering from thermoreversibly gelling schizophyllan. *Polym Gels Netw* 1998;5:541–59. [https://doi.org/10.1016/S0966-7822\(97\)00027-0](https://doi.org/10.1016/S0966-7822(97)00027-0).
- [92] Richtering HW, Gagnon KD, Lenz RW, Fuller RC, Winter HH. Physical gelation of a bacterial thermoplastic elastomer. *Macromolecules* 1992;25:2429–33. <https://doi.org/10.1021/ma00035a021>.
- [93] Frey MW, Cuculo JA, Khan SA. Rheology and gelation of cellulose/Ammonia/ammonium thiocyanate solutions. *J Polym Sci Part B* 1996;34:2375–81. [https://doi.org/10.1002/\(SICI\)1099-0488\(199610\)34:14<2375::AID-POLB7>3.0.CO;2-V](https://doi.org/10.1002/(SICI)1099-0488(199610)34:14<2375::AID-POLB7>3.0.CO;2-V).
- [94] Michon C, Cuvelier G, Launay B. Concentration dependence of the critical viscoelastic properties of gelatin at the gel point. *Rheol Acta* 1993;32:94–103. <https://doi.org/10.1007/BF00396681>.
- [95] Peyrelasse J, Lamarque M, Habas JP, El Bounia N. Rheology of gelatin solutions at the sol-gel transition. *Phys Rev E* 1996;53:6126–33. <https://doi.org/10.1103/PhysRevE.53.6126>.
- [96] Guenet JM. *Thermoreversible gelation of polymers and biopolymers*. Academic Press; 1992. ISBN: 0123053803.
- [97] Guenet JM. *Polymer-solvent molecular compounds*. Elsevier; 2008. ISBN: 0080451446.
- [98] Feng S, Sen PN. Percolation on elastic networks: new exponent and threshold. *Phys Rev Lett* 1984;52:216–9. <https://doi.org/10.1103/PhysRevLett.52.216>.
- [99] Gingold DB, Lobb CJ. Percolative conduction in three dimensions. *Phys Rev B* 1990;42:8220–4. <https://doi.org/10.1103/PhysRevB.42.8220>.
- [100] Arbabi S, Sahimi M. Mechanics of disordered solids. I. Percolation on elastic networks with central forces. *Phys Rev B* 1993;47:695–702. <https://doi.org/10.1103/physrevb.47.695>.
- [101] Arbabi S, Sahimi M. Absence of universality in percolation models of disordered elastic media with central forces. *J Phys A* 1988;21:L863–8. <https://doi.org/10.1088/0305-4470/21/17/008>.
- [102] Lemieux MA, Breton P, Tremblay AMS. Unified approach to numerical transfer matrix methods for disordered systems: applications to mixed crystals and to elasticity percolation. *J Physique Lett* 1985;46:1–7. <https://doi.org/10.1051/jphyslet:019850046010100>.
- [103] Day AR, Tremblay RR, Tremblay AMS. Rigid backbone: a new geometry for percolation. *Phys Rev Lett* 1986;56:2501–4. <https://doi.org/10.1103/PhysRevLett.56.2501>.
- [104] Jerald GR. Ph.D. thesis. University of Minnesota; 1985 (unpublished).
- [105] Feng S, Thorpe MF, Garboczi E. Effective-medium theory of percolation on central-force elastic networks. *Phys Rev B* 1985;31:276–80. <https://doi.org/10.1103/PhysRevB.31.276>.
- [106] Garboczi E, Thorpe MF. Effective-medium theory of percolation on central-force elastic networks. II. Further results. *Phys Rev B* 1985;31:7276–81. <https://doi.org/10.1103/PhysRevB.31.7276>.
- [107] Garboczi E, Thorpe MF. Density of states for random-central-force elastic networks. *Phys Rev B* 1985;32:4513–8. <https://doi.org/10.1103/PhysRevB.32.4513>.
- [108] Garboczi E, Thorpe MF. Effective-medium theory of percolation on central-force elastic networks. III. The super-elastic problem. *Phys Rev B* 1986;33:3289–94. <https://doi.org/10.1103/PhysRevB.33.3289>.
- [109] Thorpe MF, Garboczi E. Site percolation on central-force elastic networks. *Phys Rev B* 1987;35:8579–86. <https://doi.org/10.1103/PhysRevB.35.8579>.
- [110] Kantor Y, Webman I. Elastic properties of random percolating systems. *Phys Rev Lett* 1984;52:1891–4. <https://doi.org/10.1103/PhysRevLett.52.1891>.
- [111] Feng S, Sen PN, Halperin BI, Lobb CJ. Percolation on two-dimensional elastic networks with rotationally invariant bond-bending forces. *Phys Rev B* 1984;30:5386–9. <https://doi.org/10.1103/PhysRevB.30.5386>.
- [112] Feng S, Sahimi M. Position-space renormalization for elastic percolation networks with bond-bending forces. *Phys Rev B* 1985;31:1671–3. <https://doi.org/10.1103/PhysRevB.31.1671>.
- [113] Bergman D. Elastic moduli near percolation: universal ratio and critical exponent. *Phys Rev B* 1985;31:1696–8. <https://doi.org/10.1103/PhysRevB.31.1696>.
- [114] Sahimi M. Relation between the critical exponent of elastic percolation networks and the conductivity and geometrical exponents. *J Phys C* 1986;19:L79–83. <https://doi.org/10.1088/0022-3719/19/4/004>.
- [115] Roux S. Relation between elastic and scalar transport exponent in percolation. *J Phys A* 1986;19:L351–6. <https://doi.org/10.1088/0305-4470/19/6/010>.
- [116] Zabolitzky JG, Bergman DJ, Stauffer D. Precision calculation of elasticity for percolation. *J Stat Phys* 1986;44:211–3. <https://doi.org/10.1007/BF01010913>.
- [117] Arbabi S, Sahimi M. Elastic properties of three-dimensional percolation networks with stretching and bond-bending forces. *Phys Rev B* 1988;38:7173–6. <https://doi.org/10.1103/PhysRevB.38.7173>.
- [118] Benguigui L. Experimental study of the elastic properties of a percolating system. *Phys Rev Lett* 1984;53:2028–30. <https://doi.org/10.1103/PhysRevLett.53.2028>.
- [119] Deptuck D, Harrison JP, Zawadzki P. Measurement of elasticity and conductivity of a three-dimensional percolation system. *Phys Rev Lett* 1985;54:913–7. <https://doi.org/10.1103/PhysRevLett.54.913>.
- [120] Woignier T, Phalippou J, Sempere R, Pelous J. Analysis of the elastic behaviour of silica aerogels taken as a percolating system. *J Phys France* 1988;49:289–93. <https://doi.org/10.1051/jphys:01988004902028900>.
- [121] Gauthier-Manuel B, Guyon E, Roux S, Gits S, Lefaucheur F. Critical viscoelastic study of the gelation of silica particles. *J Phys France* 1987;48:869–75. <https://doi.org/10.1051/jphys:01987004805086900>.
- [122] Tokita M, Niki R, Hikichi K. Critical behavior of modulus of gel. *J Chem Phys* 1985;83:2583–6. <https://doi.org/10.1063/1.449848>.
- [123] Devreux F, Boillot JP, Chapat F, Malier L, Axelos MAV. Crossover from scalar to vectorial percolation in silica gelation. *Phys Rev E* 1993;47:2689–94. <https://doi.org/10.1103/PhysRevE.47.2689>.
- [124] Thorpe MF. Continuous deformations in random networks. *J Non-Cryst Solids* 1983;57:355–70. [https://doi.org/10.1016/0022-3093\(83\)90424-6](https://doi.org/10.1016/0022-3093(83)90424-6).
- [125] Thorpe MF. Rigidity percolation in glassy structures. *J Non-Cryst Solids* 1985;76:109–16. [https://doi.org/10.1016/0022-3093\(85\)90056-0](https://doi.org/10.1016/0022-3093(85)90056-0).
- [126] He H, Thorpe MF. Elastic properties of glasses. *Phys Rev Lett* 1985;54:2107–10. <https://doi.org/10.1103/PhysRevLett.54.2107>.
- [127] Plischke M, Joos B. Entropic elasticity of diluted central force networks. *Phys Rev Lett* 1998;80:4907–10. <https://doi.org/10.1103/PhysRevLett.80.4907>.
- [128] Plischke M, Vernon DC, Joos B, Zhou Z. Entropic rigidity of randomly diluted two- and three-dimensional networks. *Phys Rev E* 1999;60:3129–35. <https://doi.org/10.1103/PhysRevE.60.3129>.
- [129] Plischke M. Critical behavior of entropic shear rigidity. *Phys Rev E* 2006;73:061406. <https://doi.org/10.1103/PhysRevE.73.061406>.
- [130] Farago O, Kantor Y. Entropic elasticity of two-dimensional self-avoiding percolation systems. *Phys Rev Lett* 2000;85:2533–6. <https://doi.org/10.1103/PhysRevLett.85.2533>.
- [131] Mason TG, Weitz DA. Linear viscoelasticity of colloidal hard sphere suspensions near the glass transition. *Phys Rev Lett* 1995;75:2770–3. <https://doi.org/10.1103/PhysRevLett.75.2770>.
- [132] Segre PN, Prasad V, Schofield AB, Weitz DA. Glasslike kinetic arrest at the colloidal-gelation transition. *Phys Rev Lett* 2001;86:6042–5. <https://doi.org/10.1103/PhysRevLett.86.6042>.
- [133] Petekidis G, Vlassopoulos D, Pusey PN. Yielding and flow of sheared colloidal glasses. *J Phys Condens Matter* 2004;16:S955–63. <https://doi.org/10.1088/0953-8984/16/38/013>.
- [134] Bonn D, Coussot P, Huynh HT, Bertrand F, Debregeas G. Rheology of soft glassy materials. *Europhys Lett* 2002;59:786–92. <https://doi.org/10.1103/PhysRevLett.78.2020>.
- [135] Joshi YM, Reddy GRK. Aging in a colloidal glass in creep flow: time-stress superposition. *Phys Rev E* 2008;77:021501. <https://doi.org/10.1103/PhysRevE.77.021501>.
- [136] Joshi YM, Shahin A, Cates ME. Delayed solidification of soft glasses: new experiments, and a theoretical challenge. *Faraday Discuss* 2012;158:313–24. <https://doi.org/10.1039/C2FD20005H>.
- [137] Negi A, Osuji C. Dynamics of a colloidal glass during stress-mediated structural arrest. *Europhys Lett* 2010;90:28003. <https://doi.org/10.1209/0295-5075/90/28003>.
- [138] Negi A, Osuji C. Time-resolved viscoelastic properties during structural arrest and aging of a colloidal glass. *Phys Rev E* 2010;82:031404. <https://doi.org/10.1103/PhysRevE.82.031404>.
- [139] Meakin P. Formation of fractal clusters and networks by irreversible diffusion-limited aggregation. *Phys Rev Lett* 1983;51:1119–22. <https://doi.org/10.1103/PhysRevLett.51.1119>.
- [140] Kolb M, Botet R, Jullien R. Scaling of kinetically growing clusters. *Phys Rev Lett* 1983;51:1123–6. <https://doi.org/10.1103/PhysRevLett.51.1123>.
- [141] Meakin P. Diffusion-controlled Cluster formation in two, three, and four dimensions. *Phys Rev A* 1983;27:604–7. <https://doi.org/10.1103/PhysRevA.27.604>.
- [142] Vicsek T, Family F. Dynamic scaling for aggregation of clusters. *Phys Rev Lett* 1984;52:1669–72. <https://doi.org/10.1103/PhysRevLett.52.1669>.
- [143] Kolb M, Jullien R. Chemically limited versus diffusion limited aggregation. *J Physique Lett* 1984;45:977–81. <https://doi.org/10.1051/jphyslet:019840045020097700>.
- [144] Jullien R, Kolb M. Hierarchical model for chemically limited cluster cluster aggregation. *J Phys A* 1984;17:L639. <https://doi.org/10.1088/0305-4470/17/12/003>.
- [145] Brown WD, Ball RC. Computer simulation of chemically limited aggregation. *J Phys A* 1985;18:L517–21. <https://doi.org/10.1088/0305-4470/18/9/006>.
- [146] Family F, Meakin P, Vicsek T. Cluster size distribution in chemically controlled cluster-cluster aggregation. *J Chem Phys* 1985;83:4144–50. <https://doi.org/10.1063/1.449079>.
- [147] Meakin P, Vicsek T, Family F. Dynamic cluster-size distribution in cluster-cluster aggregation: effects of cluster diffusivity. *Phys Rev B* 1985;31:564–8. <https://doi.org/10.1103/PhysRevB.31.564>.
- [148] Ball RC, Weitz DA, Witten TA, Leyvraz F. Universal kinetics in reaction-limited aggregation. *Phys Rev Lett* 1987;58:274–7. <https://doi.org/10.1103/PhysRevLett.58.274>.

- [149] Meakin P, Family F. Structure and kinetics of reaction-limited aggregation. *Phys Rev A* 1988;38:2110–23. <https://doi.org/10.1103/PhysRevA.38.2110>.
- [150] Meakin P. Fractal Aggregates. *Adv Colloid Interf Sci* 1988;28:249–331. [https://doi.org/10.1016/0001-8686\(87\)80016-7](https://doi.org/10.1016/0001-8686(87)80016-7).
- [151] Meakin P. Aggregation kinetics. *Phys Scr* 1992;46:295–331. <https://doi.org/10.1088/0031-8949/46/4/002>.
- [152] Jullien R, Kolb M, Botet R. Aggregation by kinetic clustering of clusters in dimensions $D > 2$. *J Physique Lett* 1984;45:211–6. <https://doi.org/10.1051/jphyslet:01984004505021100>.
- [153] Weitz DA, Oliveria M. Fractal structures formed by kinetic aggregation of aqueous gold colloids. *Phys Rev Lett* 1984;52:1433–7. <https://doi.org/10.1103/PhysRevLett.52.1433>.
- [154] Weitz DA, Huang JS, Lin MY, Sung J. Dynamics of diffusion-limited kinetic aggregation. *Phys Rev Lett* 1985;53:1657–60. <https://doi.org/10.1103/PhysRevLett.53.1657>.
- [155] Weitz DA, Huang JS, Lin MY, Sung J. Limits of the fractal dimension for irreversible kinetic aggregation of gold colloids. *Phys Rev Lett* 1985;54:1416–9. <https://doi.org/10.1103/PhysRevLett.54.1416>.
- [156] Dimon P, Sinha SK, Weitz DA, Safinya CR, Smith GS, Varady WA, et al. Structure of aggregated gold colloids. *Phys Rev Lett* 1986;57:595–8. <https://doi.org/10.1103/PhysRevLett.57.595>.
- [157] Weitz DA, Lin MY. Dynamic scaling of Cluster-mass distributions in kinetic colloidal aggregation. *Phys Rev Lett* 1986;57:2037–40. <https://doi.org/10.1103/PhysRevLett.57.2037>.
- [158] Lin MY, Lindsay HM, Weitz DA, Ball RC, Klein R, Meakin P. Universality in colloidal aggregation. *Nature* 1989;339:360–2. <https://doi.org/10.1038/339360a0>.
- [159] Martin JE, Schaefer DW. Dynamics of fractal colloidal aggregates. *Phys Rev Lett* 1984;53:2457–60. <https://doi.org/10.1103/PhysRevLett.53.2457>.
- [160] Shaeffer DW, Martin JE, Wiltzius P, Cannell DS. Fractal geometry of colloidal aggregates. *Phys Rev Lett* 1984;52:2371–5. <https://doi.org/10.1103/PhysRevLett.52.2371>.
- [161] Aubert C, Cannell DS. Restructuring of colloidal silica aggregates. *Phys Rev Lett* 1986;56:738–41. <https://doi.org/10.1103/PhysRevLett.56.738>.
- [162] Dietler G, Aubert C, Cannell DS, Wiltzius P. Gelation of colloidal silica. *Phys Rev Lett* 1986;57:3117–20. <https://doi.org/10.1103/PhysRevLett.57.3117>.
- [163] Buscall R, Mills PDA, Goodwin JW, Lawson DW. Scaling behavior of the rheology of aggregate networks. *J Chem Soc Faraday Trans 1* 1988;84:4249–60. <https://doi.org/10.1039/F19888404249>.
- [164] de Groot JV, Macosko CW. Dynamic properties of model filled polymer melt in the linear viscoelastic region. *Theoretical and applied. Rheology* 1992;1:339–41 [eBook ISBN: 9781483294162].
- [165] Verduin H, Dhont JKG. Phase diagram of a model adhesive hard-sphere dispersion. *J Colloid Interface Sci* 1995;72:425–37. <https://doi.org/10.1006/jcis.1995.1273>.
- [166] Cao XJ, Cummins HZ, Morris JF. Structural and rheological evolution of silica nanoparticle gels. *Soft Matter* 2010;6:5425–33. <https://doi.org/10.1039/C0SM00433B>.
- [167] Martin JE, Schaefer DW, Hurd AJ. Fractal geometry of vapor-phase aggregates. *Phys Rev A* 1986;33:3540–3. <https://doi.org/10.1103/PhysRevA.33.3540>.
- [168] Krall AH, Weitz DA. Internal dynamics and elasticity of fractal colloidal gels. *Phys Rev Lett* 1998;80:778–81. <https://doi.org/10.1103/PhysRevLett.80.778>.
- [169] Sonntag RC, Russel WB. Elastic properties of flocculated networks. *J Colloid Interface Sci* 1987;116:485–9. [https://doi.org/10.1016/0021-9797\(87\)90144-5](https://doi.org/10.1016/0021-9797(87)90144-5).
- [170] Bolle G, Cametti C, Codastefano P, Tartaglia P. Kinetics of salt-induced aggregation in polystyrene lattices studied by quasi elastic light scattering. *Phys Rev A* 1987;35:837–41. <https://doi.org/10.1103/PhysRevA.35.837>.
- [171] Krall AH, Huang Z, Weitz DA. Dynamics of density fluctuations in colloidal gels. *Phys A* 1997;235:19–33. [https://doi.org/10.1016/S0378-4371\(96\)00325-1](https://doi.org/10.1016/S0378-4371(96)00325-1).
- [172] Carpineti M, Giglio M. Transition from Semiorde to disorder in the aggregation of dense colloidal solutions. *Phys Rev Lett* 1993;70:3828–31. <https://doi.org/10.1103/PhysRevLett.70.3828>.
- [173] Carpineti M, Giglio M. Spinodal-type dynamics in fractal aggregation of colloidal clusters. *Phys Rev Lett* 1992;68:3327–30. <https://doi.org/10.1103/PhysRevLett.68.3327>.
- [174] Shih WH, Shih WY, Kim SI, Liu J, Aksay IA. Scaling behavior of the elastic properties of colloidal gels. *Phys Rev A* 1990;42:4772–80. <https://doi.org/10.1103/PhysRevA.42.4772>.
- [175] Stein P, Assfalg N, Finkelmann H, Martinoty P. Shear modulus of polydomain, mono-domain and non-mesomorphic side-chain elastomers: influence of the nematic order. *Eur Phys J E* 2001;4:255–62. <https://doi.org/10.1140/epje/i2003-10154-y>.
- [176] Shih WY, Liu J, Shih WH, Aksay I. Aggregation of colloidal particles with a finite interparticle attraction energy. *J Stat Phys* 1991;62:961–84. <https://doi.org/10.1007/BF01128171>.
- [177] Haw MD, Sievwright M, Poon WCK, Pusey PN. Cluster-cluster gelation with finite bond energy. *Adv Colloid Interf Sci* 1995;62:1–16. [https://doi.org/10.1016/0001-8686\(95\)00260-W](https://doi.org/10.1016/0001-8686(95)00260-W).
- [178] Liu AJ, Nagel SR. Jamming is not just cool any more. *Nature* 1998;396:21–2. <https://doi.org/10.1038/23819>.
- [179] Lois G, Blawdziewicz J, O'Hern CS. Jamming in attractive granular media. *Proc Appl Math Mech* 2007;7:1090605–6. <https://doi.org/10.1002/pamm.200700510>.
- [180] Lois G, Blawdziewicz J, O'Hern CS. Jamming transition and new percolation universality classes in particulate systems with attraction. *Phys Rev Lett* 2008;100:028001. <https://doi.org/10.1103/PhysRevLett.100.028001>.
- [181] van Hecke M. Jamming of soft particles: geometry, mechanics. Scaling and isotaticity. *J Phys* 2010;22:033101. <https://doi.org/10.1088/0953-8984/22/3/033101>.
- [182] Ciamarra MP, Nicodemi M, Coniglio A. Recent results on the jamming phase diagram. *Soft Matter* 2010;6:2871–4. <https://doi.org/10.1039/B926810C>.
- [183] Ikeda A, Berthier L, Sollich P. Unified study of glass and jamming rheology in soft particle systems. *Phys Rev Lett* 2012;109:018301. <https://doi.org/10.1103/PhysRevLett.109.018301>.
- [184] Ikeda A, Berthier L, Sollich P. Disentangling glass and jamming physics in the rheology of soft materials. *Soft Matter* 2013;9:7669–83. <https://doi.org/10.1039/C3SM50503K>.
- [185] Herzhaft B, Kakadjian S, Moan M. Measurement and modeling of the flow behavior of aqueous foams using a recirculating pipe rheometer. *Colloids Surf A Physicochem Eng Asp* 2005;263:153–64. <https://doi.org/10.1016/j.colsurfa.2005.01.012>.
- [186] Mason TG, Bibette J, Weitz DA. Yielding and flow of monodisperse emulsions. *J Colloid Interface Sci* 1996;179:439–48. <https://doi.org/10.1006/jcis.1996.0235>.
- [187] Jacquin H, Berthier L, Zamponi F. Microscopic mean-field theory of the jamming transition. *Phys Rev Lett* 2011;106:135702.
- [188] Kroy K, Cates ME, Poon WCK. Cluster mode-coupling approach to weak gelation in attractive colloids. *Phys Rev Lett* 2004;92:148302. <https://doi.org/10.1103/PhysRevLett.92.148302>.
- [189] Cates ME, Fuchs M, Kroy K, Poon WCK, Puertas AM. Theory and simulation of gelation, arrest and yielding in attracting colloids. *J Phys Condens Matter* 2004;16:S4861–75. <https://doi.org/10.1088/0953-8984/16/42/005>.
- [190] Bergenholtz J, Fuchs M. Nonergodicity transitions in colloidal suspensions with attractive interactions. *Phys Rev E* 1999;59:5706–15. <https://doi.org/10.1103/PhysRevE.59.5706>.
- [191] Fabbian L, Götze W, Sciortino F, Tartaglia P, Thiery F. Ideal glass-glass transitions and logarithmic decay of correlations in a simple system. *Phys Rev E* 1999;59:R1347–50. <https://doi.org/10.1103/PhysRevE.59.R1347>.
- [192] Fabbian L, Götze W, Sciortino F, Tartaglia P, Thiery F. Erratum: Ideal glass-glass transitions and logarithmic decay of correlations in a simple system [Phys. Rev. E 59, R1347 (1999)]. *Phys Rev E* 1999;60:2430. <https://doi.org/10.1103/PhysRevE.60.2430>.
- [193] Dawson KA, Foff G, Fuchs M, Götze W, Sciortino F, Sperl M, et al. Higher-order glass-transition singularities in colloidal systems with attractive interactions. *Phys Rev E* 2000;63:011401. <https://doi.org/10.1103/PhysRevE.63.011401>.
- [194] Dawson D. The glass paradigm for colloidal glasses, gels, and other arrested states driven by attractive interactions. *Curr Opin Colloid Interface Sci* 2002;7:218–27. [https://doi.org/10.1016/S1359-0294\(02\)00052-3](https://doi.org/10.1016/S1359-0294(02)00052-3).
- [195] Eckert T, Bartsch E. Re-entrant glass transition in a colloidal-polymer mixture with depletion attractions. *Phys Rev Lett* 2002;89:25701. <https://doi.org/10.1103/PhysRevLett.89.125701>.
- [196] Pham KN, Egelhaaf SU, Pusey PN, Poon WCK. Glasses in hard spheres with short-range attraction. *Phys Rev E* 2004;69:011503. <https://doi.org/10.1103/PhysRevE.69.011503>.
- [197] Puertas AM, Fuchs M, Cates ME. Comparative simulation study of colloidal gels and glasses. *Phys Rev Lett* 2002;88:098301. <https://doi.org/10.1103/PhysRevLett.88.098301>.
- [198] Pham KN, Petekidis G, Vlassopoulos D, Egelhaaf SU, Pusey PN, Poon WCK. Yielding of colloidal glasses. *Europhys Lett* 2006;75:624–30. <https://doi.org/10.1209/epl/i2006-10156-y>.
- [199] Koumaki N, Petekidis G. Two-step yielding in attractive colloids: transition from gels to attractive glasses. *Soft Matter* 2011;7:2456–70. <https://doi.org/10.1039/C0SM00957A>.
- [200] Anderson VJ, de Hoog EHA, Lekkerkerker HNW. Mechanisms of phase separation and aggregation in colloidal-polymer mixtures. *Phys Rev E* 2001;65:011403. <https://doi.org/10.1103/PhysRevE.65.011403>.
- [201] de Hoog EHA, Kegel WK, van Blaaderen A, Lekkerkerker HNW. Direct observation of crystallization and aggregation in a phase-separating colloidal-polymer suspension. *Phys Rev E* 2001;64:021407. <https://doi.org/10.1103/PhysRevE.64.021407>.
- [202] Dinsmore AD, Weitz DA. Direct imaging of three-dimensional structure. *J Phys Condens Matter* 2002;14:7581–97. <https://doi.org/10.1088/0953-8984/14/33/303>.
- [203] Lu PJ, Sims PA, Oki H, Macarthur JB, Weitz DA. Target-locking acquisition with real-time confocal (TARC) microscopy. *Opt Express* 2007;15:8702–12. <https://doi.org/10.1364/OE.15.008702>.
- [204] Lu PJ, Conrad JC, Wyss HM, Schofield AB, Weitz DA. Fluids of clusters in attractive colloids. *Phys Rev Lett* 2006;96:028306. <https://doi.org/10.1103/PhysRevLett.96.028306>.
- [205] Lu PJ, Zaccarelli E, Ciulla F, Schofield AB, Sciortino F, Weitz DA. Gelation of particles with short-range attraction. *Nature* 2008;453:499–503. <https://doi.org/10.1038/nature06931>.
- [206] Zaccarelli E, Lu PJ, Ciulla F, Weitz DA, Sciortino F. Gelation as arrested phase separation in short-ranged attractive colloidal-polymer mixtures. *J Phys Condens Matter* 2008;20:494242. <https://doi.org/10.1103/10.1088/0953-8984/20/49/494242>.
- [207] Terech P, Weiss RG. Molecular gels: materials with self-assembled fibrillar networks. Springer 2006; Weiss RG. The past, present, and future of molecular gels. What is the status of the field, and where is it going? *J Am Chem Soc* 2014;136:7519–30. <https://doi.org/10.1021/ja503363v>.
- [208] Guenet JM. *Organogels: Thermodynamics, structure, solvent role and properties*. Springer; 2016. ISBN: 3319331760.